Modelling decoherence in quantum spin systems

2007 J. Phys.: Condens. Matter 19 083202

(http://iopscience.iop.org/0953-8984/19/8/083202)

IOP PUBLISHING JOURNAL OF PHYSICS: CONDENSED MATTER

J. Phys.: Condens. Matter **19** (2007) 083202 (28pp) doi:10.1088/0953-8984/19/8/083202

TOPICAL REVIEW

Modelling decoherence in quantum spin systems

Wenxian Zhang[1], **N Konstantinidis**[1], **K A Al-Hassanieh**[2,3] **and V V Dobrovitski**[1]

[1] Ames Laboratory, Iowa State University, Ames, IA 50014, USA
[2] Condensed Matter Sciences Division, Oak Ridge National Laboratory, Oak Ridge, TN 37996, USA
[3] Department of Physics, University of Tennessee, Knoxville, TN 37831, USA

E-mail: slava@ameslab.gov

Received 4 October 2006, in final form 9 January 2007
Published 6 February 2007
Online at stacks.iop.org/JPhysCM/19/083202

Abstract

In this review we discuss approaches to numerical modelling of decoherence by a spin bath. We consider several popular simulation methods, briefly discussing their implementation, and analyse their advantages and drawbacks. Furthermore, we consider application of these methods to several different physical systems, demonstrating how the numerical simulations can help in understanding the details of the decoherence process in quantum spin systems. The discussion of possible interesting directions for further research concludes the review.

(Some figures in this article are in colour only in the electronic version)

Contents

1. Decoherence: fundamental and applied aspects

Currently, considerable research effort of many experimental and theoretical groups is focused on understanding, manipulating, and using quantum spin systems for new applications. Many directions are being actively explored in various areas of physics and engineering, ranging from

advanced approaches to high-sensitivity spin detection and high-precision metrology [1–3], coherent spintronics [4], to quantum computations and quantum information processing [5]. The key unifying feature of these projects is that they all utilize quantum coherence between different states of the many-spin system. In the most basic situations, such as the Datta–Das spin field-effect transistor [6], only the single-spin coherences matter. In this device, the source–drain current is modulated due to the gate-controlled rotation of an electron spin, i.e., for an electron with the spin state $a|\uparrow\rangle + be^{i\phi}|\downarrow\rangle$ the current is determined by the relative phase ϕ between the 'up' and 'down' states. In more complex situations, the many-spin coherences (the quantum phases between the states of several different electron/nuclear spins) are important. For instance, the squeezed many-spin states which are used for high-precision magnetometry [1, 2] involve complex phase relations between different quantum states of a large number of atomic spins.

So far, quite a few theoretical proposals employing the quantum coherence of electron and/or nuclear spins have already been successfully realized in practice. Among many prominent experimental advances we here mention only a few, such as (1) implementation of the quantum factorization algorithm in liquid-state NMR experiments [7]; (2) implementation of high-precision spin measurement using the spin squeezed states [2] and the quantum entanglement between spins [3]; (3) implementation of Rabi oscillations and spin-echo experiments for single electron spins in quantum dots and for two coupled electron spins [8–10]; (4) manipulation of a few-spin ensemble in a solid by magnetic resonance force microscopy (MRFM) techniques [11]. However, only a small fraction of the proposed applications has gone beyond the basic proof-of-concept experiments. The fundamental problem which limits the practical application of quantum coherence is the inevitable interaction of real many-spin systems with their environments[4]. For instance, an electron spin in a semiconductor interacts with phonons (via spin–orbit coupling), with nuclear spins (via hyperfine interaction), with magnetic defects and impurities, etc. In the course of these interactions, the subtle phase relations between the different quantum states of the system are quickly lost; this process is often called decoherence. The state of the decohered system can no longer be represented as a coherent superposition of different quantum states, but constitutes an incoherent mixture, where different states are independent of each other and are occupied with different probabilities. The nontrivial quantum properties of the system are destroyed, and the system behaves as an essentially classical object.

In order to find efficient ways of mitigating the destructive influence of decoherence, a detailed understanding of its dynamics is needed. This is why so many theoretical and experimental studies are focused on investigating the details of the decoherence process in various physical systems. However, the widespread interest in decoherence is not bounded by its importance for novel applications. Indeed, any real system is open, interacting with a large number of environmental degrees of freedom. Therefore, decoherence is a ubiquitous phenomenon, which is important for the understanding of almost any real quantum system. The destruction of quantum phases has been considered already in the early works devoted to dynamical evolution of quantum systems [12]. Later, the loss of phase memory (dephasing) emerged as an important concept in solid-state physics, in the studies of mesoscopic conductors [13, 14], and in the theory of quantum phase transitions [15]. In parallel, studies of the decay of the many-spin coherences have become an integral part of research in nuclear magnetic resonance (NMR) and electron spin resonance (ESR), largely stimulated by the development of the multiple coherence spectroscopy [16, 17] in the 1970s.

[4] The destructive influence of the environment on the coherence of quantum systems has been discovered independently and studied by many authors; a rather comprehensive list of related papers is given in [19].

Many important aspects of decoherence have been investigated in detail in atomic and optical physics, e.g. in the studies of the interaction of the coherent light with matter [18].

At the same time, the concept of decoherence plays an important role in fundamental research devoted to the foundations of quantum mechanics and the quantum measurement problem [19–22]. The basic postulate of quantum mechanics states that quantum evolution is described by unitary transformations. Since quantum mechanics is considered to be a complete theory (within the non-relativistic domain), this statement should also be true if a quantum system interacts with a measurement apparatus (which also constitutes a very large quantum system), so that the joint evolution of the system and the apparatus should also be unitary. However, the measurement postulate asserts that the process of measurement of a quantum system (the process of interaction between the system and the apparatus) is described by a sum of projectors, and therefore cannot be represented by unitary operators. Therefore, in the course of quantum measurement the initial coherent state of the system turns into an incoherent mixture, i.e. the system becomes decohered. During this stage, the system establishes quantum correlations with the measuring apparatus, and a detailed analysis of this process is essential for understanding quantum measurements [20, 21]. It is important to note here that decoherence alone cannot completely describe the measurement process. The other components needed for complete characterization of a quantum measurement are under debate, and many related questions still remain unsolved [20], but discussion of these issues is beyond the scope of the present review.

Extensive previous studies have clarified many important issues concerning decoherence in various systems. One of the major steps in this direction was the determination of an adequate description for physically relevant environments, which, on the one hand, would be sufficiently general to be applicable to the majority of real systems, and, on the other hand, would be tractable [19, 23, 24]. It is possible to imagine some very exotic environments with very peculiar properties, and some such environments may even exist in reality (e.g., in fractional quantum Hall effect systems [25]). Fortunately, it appears that the environments which are encountered most often in real physical systems under normal circumstances (such as phonons, photons, conduction electrons, etc) can be accurately described by a single model of a 'boson bath', where a large number of environmental degrees of freedom are represented as a set of independent harmonic oscillators, each being weakly coupled with the central system [19, 23]. Being the most widespread type of environment, the boson bath has attracted much attention. A number of powerful theoretical approaches can be used in this situation, and currently the model of a boson bath is understood in much detail [19]. However, later it was realized that for many situations (such as electron spins in quantum dots, nuclear spins in solid- and liquid-state NMR experiments, magnetic clusters and molecules), the main source of decoherence is the coupling of the system with the spin environment (e.g., coupling of the electron spins with the bath of nuclear spins) [26–29]. The spin bath is essentially different from the bath of harmonic oscillators, and cannot, in general, be reduced to the boson bath model [29]. On the other hand, spin baths are encountered frequently (e.g., in nuclear magnetic resonance and electron spin resonance experiments, as well as in other situations), and, in contrast with such environments as a Luttinger liquid with backscattering [25], cannot be considered as some exotic cases. Spin environments have attracted much attention recently, but, in spite of their fundamental and applied importance, a comprehensive understanding of spin-bath decoherence is lacking. Therefore, consideration of the spin environments is of particular interest for further progress in the understanding of decoherence. Decoherence induced by spin baths constitutes the main subject of the present review.

Summarizing, decoherence is a ubiquitous phenomenon, characteristic for any open physical system. Detailed understanding of this process is of fundamental interest for many

areas of physics, ranging from solid-state physics to the foundations of quantum mechanics, and different aspects of decoherence have been studied in various contexts for many decades. Beside the fundamental importance, the studies of decoherence have recently become an essential part of more applied research effort, focused on practical use of quantum coherence in spin systems. However, the impressive experimental advances in this area constitute only the first steps, and detailed understanding of decoherence in spin systems is needed for further progress. Among other sources, the decoherence induced by the spin environments is of particular interest for further progress in the understanding of decoherence; spin-bath decoherence constitutes the subject of the present review.

2. Methods for numerical modelling of decoherence

In order to rigorously describe the decoherence process, both the central system and its environment should be explicitly taken into consideration. Therefore, let us consider a central system whose dynamics is described by the Hamiltonian H_{S}, and which is coupled to the bath of external degrees of freedom (described by the Hamiltonian H_{B}) via the interaction H_{SB}, so that the composite Hamiltonian is

$$H = H_{\mathrm{S}} + H_{\mathrm{SB}} + H_{\mathrm{B}}. \tag{1}$$

We assume that the central system has been prepared in some state $|\phi_0\rangle$, and that the bath is initially in the state $|\chi_0\rangle$, so that at $t = 0$ there are no correlations between the system and the bath, and the state $|\Psi(0)\rangle$ of the composite system (the central system plus the bath) at $t = 0$ is separable, $|\Psi(0)\rangle = |\phi_0\rangle \otimes |\chi_0\rangle$. In the course of evolution, due to the system–bath coupling, the central system and the bath develop quantum correlations, and the composite wavefunction $|\Psi(t)\rangle$ is no longer separable, i.e. it cannot be decomposed into a direct product of two functions which would describe the central system and the bath as separate entities. Such quantum correlations are called entanglement: in the wavefunction $|\Psi(t)\rangle$ the state of the system cannot be separated from the state of the bath [20–22].

In most cases we are not interested in a detailed description of the bath, so it is convenient to describe the properties of the central system by the reduced density matrix $\rho_{\mathrm{S}} = \mathrm{Tr}_{\mathrm{B}} |\Psi(t)\rangle\langle\Psi(t)|$, where Tr_{B} denotes trace over the bath degrees of freedom. As is the case for any Hermitian matrix, it can be diagonalized, and represented as

$$\rho_{\mathrm{S}} = \mathrm{Tr}_{\mathrm{B}} |\Psi(t)\rangle\langle\Psi(t)| = \sum_j w_j(t)|\phi_j(t)\rangle\langle\phi_j(t)|. \tag{2}$$

Such a density matrix can be re-interpreted as an incoherent mixture[5] of different states $|\phi_j(t)\rangle$ occupied with the probabilities w_j. Obviously, coherence of the cental system is preserved only if the matrix ρ_{S} describes a pure quantum state, i.e. satisfies the condition $\rho_{\mathrm{S}}^2 = \rho_{\mathrm{S}}$. This happens only if the composite wavefunction $|\Psi\rangle$ is separable. However, when the quantum correlations are established between the central system and its environment, the matrix ρ_{S} describes a decohered mixed state.

Decoherence is a non-equilibrium many-body process, where strong quantum correlations play a central role. Its description, in general, is a problem of immense complexity. The course of the decoherence process may strongly depend on very subtle features of the system

[5] Of course, such re-interpretation raises many questions. For example, how is it possible to re-interpret the density matrix (2), which describes a single instance of a system decohered by a single instance of environment, using the incoherent mixture which implies an ensemble of systems occupying different states with different probabilities. Another interesting question arises when some of w_j are equal to each other, and the corresponding states $|\phi_j\rangle$ cannot be determined uniquely. The answers to these question are rather subtle, and some aspects are still discussed in the literature. We do not discuss them here, instead referring any interested reader to [20].

and/or the bath dynamics [30–33], such as the onset of quantum chaos in the bath [34, 35] or parity of the central system [36, 37]. Analytical studies, except for a handful of simple cases, inevitably involve some approximations. By now, several methods for approximate analysis of dynamics of an open system have been formulated. For instance, the influence of the bath can be approximately represented as a noise, classical or quantum, and the corresponding Liouville equation can be derived for the relevant system's observables [18]. In another approach, an approximate equation of motion for the reduced density matrix can be derived, known as the master equation, where the influence of the environment is represented as some non-unitary terms [38, 39]. Based on these studies, a certain 'standard picture' of the decoherence process has been developed, which greatly helps in the understanding of decoherence in general. However, for these approximate methods to be valid, one has to make rather stringent assumptions about the dynamics of the bath and/or about the properties of the system–bath interaction (e.g., very weak or very strong interaction, very fast Markovian bath or very slow quasi-static bath, etc), which are not always satisfied in reality. Accordingly, the cases where these special conditions are not present, and where the dynamics of decoherence deviates from the standard one, are of special interest, as they extend a list of possible decoherence scenarios and provide new insights in the dynamics of the decoherence process. We believe that detailed and systematic studies of such non-standard situations, which would employ both numerical and analytical tools, will make it possible in the future to reveal the common features for novel decoherence scenarios and to develop an intuitive picture for them. Numerical modelling will be of crucial help in this endeavour. Numerical studies are important for analysing the situations where the existing approximate treatments are not valid (or, at least, not obvious). The approximation-free numerical results, especially strengthened by qualitative analytical arguments, can be valuable for deeper understanding of decoherence. Moreover, such numerical simulations may be very helpful for validating the approximations which are intuitively correct but are hard to justify by purely analytical tools. In section 3 of this review, we present several examples of such numerical studies.

2.1. Direct simulations

The most direct approach to the numerical simulation of decoherence is to explicitly model the joint dynamics of the central system and the bath, starting from the basic principles of quantum mechanics. For the given composite system which contains N_S cental spins and N_B bath spins, we specify the Hamiltonians H_S, H_B, and H_{SB}, and, knowing the initial composite wavefunction $|\Psi(0)\rangle = |\phi_0\rangle \otimes |\chi_0\rangle$, we explicitly calculate $|\Psi(t)\rangle$ for any $t > 0$, thus determining the evolution of any relevant observable. This approach, obviously, does not discriminate the spins belonging to the system from the bath spins: all $N = N_S + N_B$ spins are treated on equal footings. Therefore, in this section, we will use the same notation S_k ($k = 0 \ldots N - 1$) for all spins, whether these are bath spins or central spins. A general Hamiltonian describing such a system of spins 1/2 with pairwise interactions is

$$H = \sum_k B_k^\alpha S_k^\alpha + \sum_{jm} \sum_{\alpha,\beta=x,y,z} J_{jm}^{\alpha\beta} S_j^\alpha S_m^\beta, \tag{3}$$

where B_k^α are the components of the local fields, and $J_{jm}^{\alpha\beta}$ are the spin coupling parameters. For simplicity of presentation, everywhere below we consider only spins 1/2, which is sufficient for the purposes of the present review. For similar reasons, we neglect the three-spin and higher-order interactions, which are irrelevant in most experimental situations.

To implement the direct approach described above, we expand the composite wavefunction $|\Psi\rangle$ in some orthonormal basis $|X_a\rangle$. The most direct choice is the basis set constructed as the

direct product of the individual spin states: $|X_a\rangle = |\alpha_{N-1}\alpha_{N-2}\ldots\alpha_1\alpha_0\rangle$, where $\alpha_k = 1$ if the kth spin is in the state 'up' and $\alpha_k = 0$ if this spin is in the state 'down'. There are $M = 2^N$ such basis states, so the index a runs from zero to $M-1$. Expanding the wavefunction $|\Psi\rangle$ in this basis,

$$|\Psi\rangle = \sum_{a=0}^{M-1} P_a|X_a\rangle, \tag{4}$$

we represent the state of the composite system as a set of M complex numbers P_a arranged in a one-dimensional array P. The action of any operator A on the wavefunction $|\Psi\rangle$ is reduced to some modification of the elements of this array

$$A|\Psi\rangle = \sum_{a=0}^{M-1} P_a A|X_a\rangle = \sum_{a=0}^{M-1} P'_a|X_a\rangle \tag{5}$$

where P'_a denotes the modified values of the elements of the array P. In order to describe the dynamics of the decoherence process, we need to determine the temporal evolution of $P_a(t)$.

Naively, one may represent the Hamiltonian as a matrix in the basis $|X_a\rangle$, and, after diagonalizing this matrix, express $|\Psi(t)\rangle$ via the eigenvalues E_i and the eigenvectors $|\psi_i\rangle$. However, this approach is extremely inefficient [40]. The diagonalization requires M^3 operations, and at every moment of time, in order to calculate the value of some observable $A(t)$, one must perform M^3 operations. Moreover, the sparse structure of the Hamiltonian (3) is often lost in the course of diagonalization, so the whole Hamiltonian matrix (M^2 real numbers) should be stored in the memory. As a result, the simulations with more than 10–15 spins can rarely be performed using this naive approach (unless the wavefunction $|\Psi(t)\rangle$ is artificially restricted to some sufficiently small dynamically invariant subspace of the Hamiltonian).

It is important to realize that determination of the eigenstates/eigenvalues of the Hamiltonian and modelling of the dynamical evolution are different (although closely related) problems, which require different approaches. To date, a large number of numerical methods have been designed particularly for dynamical modelling of quantum systems, e.g. in quantum chemistry. However, not all these approaches are applicable to decoherence studies. Typical quantum chemistry simulations describe the propagation of wavepackets, and most of the relevant basis states have energy close to the energy of a wavepacket. Only these relevant states should be accurately described, while an accurate description of the whole energy spectrum is excessive [41]. In contrast, for most of the decoherence simulations the initial state of the bath is usually highly disordered, so the composite wavefunction involves a large number of basis states with very different energies. This distinctive feature limits the number of methods suitable for modelling decoherence. Below, we describe two efficient approaches, the Suzuki–Trotter decomposition [42–44] and the Chebyshev polynomial expansion [40, 41, 45–47], in some detail (these are the methods used for simulations in section 3), and briefly discuss some other promising approaches to modelling dynamics of many-spin systems over substantially long periods of time.

The Suzuki–Trotter decomposition [42, 48] has acquired much popularity, due to its efficiency, conceptual simplicity, and applicability for a wide range of situations, including explicitly time-dependent Hamiltonians. Within this approach, the Hamiltonian H is subdivided into a sum of terms $H_1, \ldots, H_r, \ldots$, and the evolution operator $U = \exp(-\mathrm{i}H\delta)$ over a short timestep δ is represented via the product of $U_r = \exp(-\mathrm{i}H_r\delta_r)$, $r = 1, \ldots, R$. In the simplest case, $U = \prod_r \exp(-\mathrm{i}H_r\delta) + \mathrm{O}(\delta^2)$; more complex decompositions of higher orders can be derived as well [42, 48], e.g. up to the second order, $U = U_> U_< + \mathrm{O}(\delta^3)$, where

$$U_> = \exp(-\mathrm{i}H_1\delta/2)\exp(-\mathrm{i}H_2\delta/2)\ldots\exp(-\mathrm{i}H_R\delta/2), \tag{6}$$

$$U_< = \exp(-\mathrm{i}H_R\delta/2)\exp(-\mathrm{i}H_{R-1}\delta/2)\ldots\exp(-\mathrm{i}H_1\delta/2). \tag{7}$$

The terms H_r should be chosen in such a way that the action of the operators U_r on the wavefunction $|\Psi\rangle$ can be efficiently implemented. The simplest (although not the most economic) choice is to treat every term in equation (3) separately:

$$\exp(-\mathrm{i}B_j^\alpha S_j^\alpha t) = \cos(B_j^\alpha t/2) - 2\mathrm{i}S_j^\alpha \sin(B_j^\alpha t/2) \tag{8}$$

$$\exp(-\mathrm{i}J_{jm}^{\alpha\beta} S_j^\alpha S_m^\beta t) = \cos(J_{jm}^{\alpha\beta} t/4) - 4\mathrm{i}S_j^\alpha S_m^\beta \sin(J_{jm}^{\alpha\beta} t/4), \tag{9}$$

so that the function $|\Psi(t+\delta)\rangle$ can be obtained from $|\Psi(t)\rangle$ via a sequence of simple manipulations which are easy to implement in an efficient way, involving only the multiplication by a constant and the action of the operators S_k^α on the composite wavefunction. In general, the optimal choice of the sub-Hamiltonians H_r is dictated by many factors, such as the particular form of the Hamiltonian, requirements of vectorization or parallelization of the code, etc. The application of the operators U_r to the wavefunction $|\Psi\rangle$ does not require additional memory: the elements of the resulting vector $|\Psi_r\rangle = U_r|\Psi\rangle$ can simply replace the corresponding elements of $|\Psi\rangle$, so the Suzuki–Trotter approach requires the amount of memory which grows linearly with M. Also, the operations count per timestep is linear in M. However, as with any multistep method, the Suzuki–Trotter approach may be difficult to use for studying the decoherence dynamics during very long time intervals. In order to propagate the wavefunction $|\Psi\rangle$ over the time interval t, one divides this interval into n timesteps, each of size $\delta = t/n$, and applies the kth order Suzuki–Trotter decomposition at every timestep, thus introducing an error of order δ^{k+1} per step. The total error accumulated in the wavefunction $|\Psi(t)\rangle$ is of order $n\delta^{k+1}$, and if we require this quantity to be smaller than some predefined tolerance ϵ then we need to keep a timestep of order of $(\epsilon/t)^{1/k}$, which means that the required number of timesteps, and hence the total computation time, grows superlinearly with time as $t^{1+1/k}$, and decompositions of order $k > 4$ are rarely used.

The computation time can be noticeably reduced by using another scheme, based on the Chebyshev polynomial expansion [40, 41, 45, 46], where the computation time grows practically linearly with t. Replacement of $t^{5/4}$ (corresponding to the fourth-order Suzuki–Trotter decomposition) by t may seem to be of little advantage, but in decoherence studies one often has to simulate the system over millions of timesteps, so the use of the Chebyshev polynomials often decreases the simulation time by a factor of 10–20. However, this gain comes with a limitation: the Chebyshev polynomial expansion is applicable only to Hamiltonians which have no explicit time dependence, and its extension to time-dependent situations is nontrivial.

The Chebyshev polynomial expansion is a single-step method, which propagates the wavefunction over the time interval t in a single step. The essence of the approach is the following expression for the exponent of any operator G such that $||G|| \leqslant 1$:

$$\exp(-\mathrm{i}G\tau) = 1 + 2\sum_{k=0}^{\infty}(-\mathrm{i})^k J_k(\tau) T_k(G) \tag{10}$$

where $J_k(\tau)$ is the Bessel function of kth order and $T_k(G)$ is the Chebyshev polynomial of the operator G. Since the many-spin Hamiltonian (3) is bounded, we can find such a number E_1 that $||H|| \leqslant E_1/2$, and, by defining the rescaled Hamiltonian $G = 2H/E_1$ and the rescaled time $\tau = E_1 t/2$, use (10) for calculation of the evolution operator. The key feature of the expansion (10) is that the expansion coefficients $J_k(\tau)$ decrease superexponentially, as $(\tau/k)^k$ at large k. This means that the series can be truncated at some sufficiently large $k = K$, and the resulting error can be smaller than some pre-defined tolerance ϵ. In practice, truncation at $K = 1.5\tau$ already gives precision of 10^{-7} or better in most cases. At the same time, the Chebyshev polynomials $T_k(G)$ can be efficiently calculated using the recurrence relation

$$T_{k+1}(G) = 2GT_k(G) + T_{k-1}(G) \tag{11}$$

with $T_0(G) = 1$ and $T_1(G) = G$. Thus, the number of operations needed for calculation of every term in the series (10) grows linearly with M, and the required memory also increases linearly with M. The total operations count needed to propagate the wavefunction over the time interval t increases linearly with the truncation order K, and, correspondingly, the computation time increases practically linearly with t. Therefore, the Chebyshev polynomial expansion is very suitable for simulating the decoherence process at long times [40, 41].

In reality, however, it is not the computation time but the memory requirements which limit the application of both the Suzuki–Trotter decomposition and the Chebyshev polynomial expansion. A typical single-processor workstation addresses only about 1 Gbyte of random access memory, which means that only about $N = 25$ quantum spins can be modelled, and with increasing N, the required memory grows exponentially with N. For simulations of larger systems, with 30–40 spins, parallel multiprocessor systems are used. The elements P_a of the array P, which determine the composite wavefunction (see equation (4)), are distributed between different processes, so that the calculation of $|\Psi(t)\rangle$ includes both single-process computations and inter-process communications. The computations are performed by all processes in parallel, so the corresponding time decreases as $1/p$, where p is the number of processes. The communication time depends on the particular implementation and on the specific form of the Hamiltonian (3). For example, in a rather unfavourable situation, when every spin is coupled to all other spins via Heisenberg exchange, the communication time decreases as $(\log_2 p)^2/p$ with increasing the number of processes p. Although the communication time decreases more slowly than the computation time, nevertheless, the total amount of computation still remains much larger than the amount of communication, because N is usually much larger than $\log_2 p$. In our experience, degradation of the efficiency is tolerable for small clusters with $p = 8$–16, and becomes important when larger computers are used. However, if one needs to model larger systems, with 60–100 spins, simply increasing the amount of available memory is not a good way to go. For these simulations, different approaches have to be employed.

In order to drastically reduce the memory requirements, we need to decrease the number of the basis states needed for the description of the composite system. Therefore, we need to construct a basis which would change, in an adaptive manner, with the system's evolution, in order to provide the best possible description of $|\Psi(t)\rangle$ using the least possible number of basis states. This idea underlies numerous approximate methods in many-body physics, ranging from the classical mean-field approach to such sophisticated modern methods as for example the multi-configurational time-dependent Hartree (MCTDH) method [49, 50]. Within this method, it is assumed that the composite wavefunction $|\Psi\rangle$ can be approximated by a superposition of a relatively small number of time-dependent 'configurations', i.e. products of time-varying spin wavefunctions. While the MCTDH method is known to be efficient for modelling the boson-bath decoherence, to our knowledge, its applicability for the spin-bath decoherence (in particular, accuracy of the multi-configurational Hartree approximation) has not been studied yet.

The idea of an adaptive time-varying basis has been widely exploited recently in a different framework, within the time-dependent density matrix renormalization group (TDMRG) approach [51–53]. The density matrix renormalization group was developed initially for modelling of the equilibrium thermodynamic properties of many-body systems [54], and later it was extended to study non-equilibrium evolution. Within this method, the many-spin system is divided into subsystems, and the wavefunction for the system is constructed as a superposition of the relevant subsystems' states, chosen from Schmidt decomposition of the density matrix (hence the name of the method). These relevant states form a very suitable time-dependent adaptive basis, which accurately represents the wavefunction $|\Psi\rangle$ and at the same

time has very low dimensionality. The use of the truncated set of the basis states introduces errors in the simulations, but the accuracy can be controlled by taking a sufficiently large number of basis states. The success of the method is based on the fact that for a wide range of practically interesting systems the number of the time-dependent basis states needed for accurate representation of $|\Psi(t)\rangle$ remains relatively small. So far, in several applications, systems with 100–200 spins have been simulated using the TDMRG approach [51, 55]. However, for some sufficiently complex dynamical evolution, when all spins in the system are strongly entangled with each other, the number of required basis states may grow very rapidly with time, negating all advantages of the TDMRG method (in which case one has to resort to the Suzuki–Trotter or Chebyshev expansion methods). Detailed studies of such situations are yet to be performed.

2.2. Coherent-state approach

All limitations of the direct approaches mentioned above stem from one fundamental problem: the dimensionality of the Hilbert space of a many-spin system grows exponentially with the number of spins, and numerical modelling of many-dimensional space is very hard. However, Monte Carlo (MC) methods have been developed to solve this very problem, and it would be extremely beneficial to find a way of applying random sampling for decoherence simulations [56]. For the MC sampling to be useful, the evolution operator should be represented as a sum of positively definite transition probabilities (possibly with different weights ascribed to different trajectories). This condition is often satisfied for the imaginary-time (i.e., finite-temperature) simulations, but even in this case, for various many-fermion or frustrated many-spin systems, the trajectories with both positive and negative 'probabilities' should be taken into account (the so-called sign problem) [57]. When the number of the trajectories with negative 'probabilities' is sufficiently large, the statistical error of the MC simulations increases exponentially, making the MC sampling practically useless. In the case of dynamical non-equilibrium simulations, the severe sign problem is always present. Indeed, a matrix element of the evolution operator between some orthonormal basis states $|X_a\rangle$ and $|X_b\rangle$ is

$$\langle X_b|\exp(-\mathrm{i}Ht)|X_a\rangle = \sum_j \langle X_a|\psi_j\rangle\langle\psi_j|X_b\rangle \exp(-\mathrm{i}E_j t) \tag{12}$$

where $|\psi_j\rangle$ and E_j denote, correspondingly, the eigenstates and eigenenergies of the compound Hamiltonian, so the transition from $|X_b\rangle$ to $|X_a\rangle$ is a superposition of many complex 'probabilities' which have, in general, comparable absolute values.

Nevertheless, it is possible to construct an approximate, but extremely accurate, sampling procedure, suitable for simulating the spin-bath decoherence, which employs the positively definite transition probabilities and allows modelling systems with many thousands of spins on a single-processor workstation [58]. In order to achieve that, a basis of *non-orthogonal* coherent states should be used [59, 60]. Traditionally, spin coherent states are used in solid-state physics for derivation of the semiclassical approximation and for construction of the spin path integrals. As we show below and in section 3, the coherent-state representations of the density matrix [18, 61, 62], widely used in quantum optics, may constitute a powerful tool for studying spin-bath decoherence.

The coherent state for spin J is defined as $|\mu\rangle = \mathcal{N}\sum_{m=0}^{2J}[(2J)!/(m!(2J-m)!)]^{1/2}\mu^m|J-m\rangle$, where $\mathcal{N} = (1+|\mu|^2)^{-J}$ is the normalization constant [59, 60]. For a spin 1/2, the coherent state has a simple form

$$|\mu\rangle = \cos(\theta/2)|\uparrow\rangle + \sin(\theta/2)\mathrm{e}^{\mathrm{i}\phi}|\downarrow\rangle, \tag{13}$$

where we have used the parameterization $\mu = \tan(\theta/2)e^{i\phi}$. The basis of coherent states is overcomplete, so the expansion of an operator in this basis is not uniquely defined. In particular, any Hermitian operator A can be represented in a *diagonal* form using only the real matrix elements, i.e. it is possible to choose a real-valued function $\tilde{A}(\theta, \phi)$ such that

$$A = \int_{\Omega} \tilde{A}(\theta, \phi)|\mu\rangle\langle\mu| \sin\theta \, d\theta \, d\phi, \tag{14}$$

where the integration is performed over the sphere [18, 61, 62]. Note that $\tilde{A}(\theta, \phi) \neq \langle\theta, \phi|A|\theta, \phi\rangle$, and the function $\tilde{A}(\theta, \phi)$ is not necessarily positive. It is also important to note that the choice of $\tilde{A}(\theta, \phi)$ is not unique: any linear combination of spherical harmonics $Y_l^m(\theta, \phi)$ of the order $l > 2J$ can be added to it, without changing the operator A. The density matrix, obviously, can also be written in a diagonal form (14) using an appropriate function $P(\theta, \phi)$; this representation is called the P-representation.

For a many-spin system, the P-representation of a composite density matrix has a remarkable form:

$$\rho = \int P(\{\theta_j, \phi_j\}) \bigotimes_{j=0}^{N-1} |\mu_j\rangle\langle\mu_j| \prod_{j=0}^{N} \sin\theta_j \, d\theta_j \, d\phi_j, \tag{15}$$

where $\{\theta_j, \phi_j\}$ denotes the set of all $\theta_0, \ldots, \theta_{N-1}$ and $\phi_0, \ldots, \phi_{N-1}$. Within the P-representation, the 'matrix part' of the density matrix has a mean-field-like form: it is a direct product of the matrices of the individual spins, while all many-body aspects of composite system are completely described by the single function $P(\{\theta_j, \phi_j\})$. However, in contrast with the mean-field approximation, the representation (15) is exact. Using the P-representation, the quantum-mechanical average $x = \mathrm{Tr}(\rho(t)X)$ of any observable X can be calculated by simple integration,

$$x = \int P(\{\theta_j, \phi_j\}, t) \bigotimes_{j=0}^{N-1} \langle\mu_j|X|\mu_j\rangle \prod_{j=0}^{N-1} \sin\theta_j \, d\theta_j \, d\phi_j. \tag{16}$$

Therefore, the function P possesses all the good properties of the probability density, and we only need to find a way to accurately model its evolution.

Obviously, direct solution of the complex partial differential equation for $P(\{\theta_j, \phi_j\}, t)$ is impossible for a large number of spins, and a Monte Carlo sampling is the natural way to go. We initially generate many samples of the random vector $(\theta_0^{(m)}, \ldots, \theta_{N-1}^{(m)}, \phi_0^{(m)}, \ldots, \phi_{N-1}^{(m)})$ distributed according to the probability distribution $P(\{\theta_j, \phi_j\}, 0)$ (the index $m = 1, \ldots, M$ enumerates the different samples). Then we propagate all the sample vectors in time, so that every initial sample vector $(\theta_0^{(m)}, \ldots, \theta_{N-1}^{(m)}, \phi_0^{(m)}, \ldots, \phi_{N-1}^{(m)})$ after a period of time t evolves into a vector $(\Theta_0^{(m)}(t), \ldots, \Theta_{N-1}^{(m)}(t), \Phi_0^{(m)}(t), \ldots, \Phi_{N-1}^{(m)}(t))$. If the equations of motion for all variables $\Theta_j^{(m)}(t)$ and $\Phi_j^{(m)}(t)$ are chosen correctly, then the distribution function $P(\{\theta_j, \phi_j\}, t)$ coincides with the distribution $P(\Theta_j(t), \Phi_j(t))$. The value $x = \mathrm{Tr}(\rho(t)X)$ of any observable X can be calculated as an average over the samples:

$$x = \frac{1}{M} \sum_{m=1}^{M} \bigotimes_{j=0}^{N-1} \langle\Theta_j^{(m)}, \Phi_j^{(m)}|X|\Theta_j^{(m)}, \Phi_j^{(m)}\rangle \sin\Theta_j^{(m)}. \tag{17}$$

If we manage to ensure that the P-function is positively definite (we show how to do this below) then the MC sampling would allow accurate simulations for thousands of spins.

But first let us find the equations of motion (EOMs) for $\Theta_j(t)$ and $\Phi_j(t)$. In quantum optics, the EOMs for relevant bosonic variables are derived in a somewhat intricate way, by using so-called positive P-representation, deriving the Fokker–Planck equation for the

corresponding P-function and transforming it into the Langevin equations, solving the latter by MC sampling [63–65]. For spin systems, to our knowledge, such an approach has not been implemented yet due to a number of difficulties. We are using a different approach, differentiating both sides of equation (15) with time and, using the fact that $\mathrm{d}P/\mathrm{d}t = \sum_j (\partial P/\partial \Theta_j)\,\mathrm{d}\Theta_j/\mathrm{d}t + (\partial P/\partial \Phi_j)\,\mathrm{d}\Phi_j/\mathrm{d}t$, we choose expressions for $\mathrm{d}\Theta_j/\mathrm{d}t$ and $\mathrm{d}\Phi_j/\mathrm{d}t$ such that they satisfy the resulting equation.

To illustrate how this approach works, let us consider a model which will be considered in section 3.1, where a single central spin $\mathbf{S}_0$ is coupled to a bath of nuclear spins $\mathbf{S}_1 \ldots \mathbf{S}_N$ via Heisenberg interactions:

$$H = \sum_k A_k \mathbf{S}_0 \mathbf{S}_k. \tag{18}$$

To begin, let us study one term in this Hamiltonian, i.e. we consider two spins 1/2 (the central spin and the kth bath spin) coupled by the isotropic Heisenberg interaction $\mathcal{H}_k = A_k \mathbf{S}_0 \mathbf{S}_k$. The most general form for the two-spin density matrix is $\rho = w_{00}\mathbf{1}_0\mathbf{1}_k + w_{0\alpha}\mathbf{1}_0\sigma_k^\alpha + w_{\beta 0}\sigma_0^\beta \mathbf{1}_k + w_{\lambda\nu}\sigma_0^\lambda \sigma_k^\nu$, where $\alpha = x, y, z$ (and similarly for other Greek indices), σ_0^α and σ_k^β denote the Pauli matrices for the 0th and the kth spin, respectively, and $\mathbf{1}_0$ ($\mathbf{1}_k$) denotes the unity matrix for the 0th (kth) spin. Here and below, we assume summation over the repeated indices. From von Neumann's equation $\dot\rho(t) = \mathrm{i}[\rho(t), \mathcal{H}]$, we obtain $\dot w_{00}(t) = 0$ (which expresses the fact that $\mathrm{Tr}\rho(t) = 1$), and

$$\begin{aligned} \dot w_{0\gamma}(t) &= \frac{A_k}{2}\epsilon_{\alpha\beta\gamma} w_{\alpha\beta}(t), \qquad \dot w_{\gamma 0}(t) = -\frac{A_k}{2}\epsilon_{\alpha\beta\gamma} w_{\alpha\beta}(t), \\ \dot w_{\alpha\beta}(t) &= \frac{A_k}{2}\epsilon_{\alpha\beta\gamma}[w_{\gamma 0}(t) - w_{0\gamma}(t)], \end{aligned} \tag{19}$$

where $\epsilon_{\alpha\beta\gamma}$ is a completely antisymmetric unity tensor (permutation symbol). On the other hand, from the P-representation (15) it is easy to find that $P(\{\theta_0, \phi_0, \theta_k, \phi_k\}, t) = p_{00}(t) + p_{0\alpha}(t)c_k^\alpha + p_{\beta 0}(t)c_0^\beta + p_{\lambda\nu}(t)c_0^\lambda c_k^\nu$, where $p_{00} = (1/4\pi^2)w_{00}$, $p_{0\alpha} = (3/4\pi^2)w_{0\alpha}$, $p_{\alpha 0} = (3/4\pi^2)w_{\alpha 0}$, and $p_{\alpha\beta} = (9/4\pi^2)w_{\alpha\beta}$. Here, we have used the shorthand notations $c_0^x = \sin\theta_0\cos\phi_0$, $c_0^y = \sin\theta_0\sin\phi_0$, $c_0^z = \cos\theta_0$ (and similarly for c_k^x, c_k^y, c_k^z). Note, as we mentioned above, that the spherical harmonics of the order two and higher in $P(\{\theta_0, \phi_0, \theta_k, \phi_k\})$ are irrelevant: they do not change the density matrix.

Let us assume that the EOMs for (Θ_0, Φ_0) and (Θ_k, Φ_k) can be written in a form resembling the motion of classical spins. Introducing the shorthand notations $C_0^x = \sin\Theta_0\cos\Phi_0$, $C_0^y = \sin\Theta_0\sin\Phi_0$, $C_0^z = \cos\Theta_0$ (and similarly for C_k^x, C_k^y, C_k^z), we assume that the EOMs have the form

$$\dot{\mathbf{C}}_0 = g_1[\mathbf{C}_k \times \mathbf{C}_0], \qquad \dot{\mathbf{C}}_k = -g_2[\mathbf{C}_k \times \mathbf{C}_0], \tag{20}$$

where g_1 and g_2 are some constants to be determined. Substituting these assumed EOMs into the probability distribution $P(\{\Theta_0(t), \Phi_0(t), \Theta_k(t), \Phi_k(t)\}) = P_{00} + P_{0\alpha}C_k^\alpha + P_{\beta 0}C_0^\beta + P_{\lambda\nu}C_0^\lambda C_k^\nu$, we find that the evolution of the corresponding density matrix is described by the equations

$$\begin{aligned} \dot w_{0\gamma}(t) &= -g_2\epsilon_{\alpha\beta\gamma} w_{\alpha\beta}(t), \qquad \dot w_{\gamma 0}(t) = g_1\epsilon_{\alpha\beta\gamma} w_{\alpha\beta}(t), \\ \dot w_{\alpha\beta}(t) &= (1/3)\epsilon_{\alpha\beta\gamma}[g_2 w_{0\gamma}(t) - g_1 w_{\gamma 0}(t)], \end{aligned} \tag{21}$$

and $\dot w_{00}(t) = 0$. Comparing the equations (19) and (21), one may see that they are incompatible, and the assumed EOMs (20) should be discarded. However, we are interested only in $w_{\gamma 0}(t)$, since only this term determines the value of $\mathbf{S}_0(t)$. By choosing $g_1 = g_2 = g = A_k\sqrt{3}/2$, and differentiating (19) and (21) with respect to time once more, we see that they produce the same result:

$$\ddot w_{\gamma 0}(t) = -\ddot w_{0\gamma}(t) = (A_k^2/2)(w_{0\gamma} - w_{\gamma 0}). \tag{22}$$

Thus, the coefficients $w_{\gamma 0}(t)$ produced by the assumed EOMs (20) and by the exact equations (19) coincide, provided that the initial conditions $w_{\gamma 0}(0)$ and $\dot{w}_{\gamma 0}(0)$ also coincide, which implies that all $w_{\alpha\beta}(0)$ should be equal to zero. The latter condition means that the method described above is applicable only to completely disordered baths. This limitation is not catastrophic, and is satisfied in many experimentally relevant situations. On the other hand, the advantages of the present approach are significant. It allows modelling of very large baths (tens of thousand of spins) with very modest computer resources, and the equations of motion are extremely simple: one just has to replace the coupling constants A_k by $A_k\sqrt{3}/2$, and simulate the motion of classical spins.

It is important to note that the coherent-state approach described above is *not* equivalent to a standard semiclassical approximation. The easiest way to demonstrate that is to consider the situation of unequal spins 1 and 1/2 ($S_0 = 1$ and $S_k = 1/2$). The analysis above gives $g_1 = A_k\sqrt{3}/2$, $g_2 = A_k\sqrt{7}/2$, while the semiclassical approach would give $g_1 = A_k\sqrt{3}/2$, $g_2 = A_k\sqrt{2}$. Furthermore, the initial conditions are different: for instance, if the central spin 1/2 is initially directed along the z-axis then the initial density matrix $\rho = 2^{-N_B}|\uparrow\rangle\langle\uparrow| \bigotimes_{k=1}^{N_B} \mathbf{1}_k$, which means that the initial P-function is $P(\{\theta_j, \phi_j\}, 0) = (4\pi)^{-N}(1 + 3\cos\theta_0)$, while the semiclassics would require the central spin to be directed up, and the corresponding probability distribution is $p(\{\theta_j, \phi_j\}, 0) = (4\pi)^{-N}\delta(\cos\theta_0 - 1)$, where $\delta(\ldots)$ is the Dirac delta-function.

The final problem which has to be solved is how to make the function $P(\{\theta_j, \phi_j\})$ positively definite. In quantum optics, for modelling the bosonic systems, a more general representation (positive P-representation) is used for this purpose. For spin systems, where the use of positive-P representation is associated with a number of difficulties, we choose a simpler approach: instead of using the original P-function, which is not positively definite, we use the function $P' = a + bP$ where the constants a and b are chosen to make $P'(\{\theta_j, \phi_j\})$ positive everywhere and, at the same time, to keep correct normalization. This trick is equivalent to replacing the original density matrix ρ by $\rho' = a\mathbf{1} + b\rho$, where $\mathbf{1}$ is the unity operator which is not affected by any unitary evolution, so that its contribution to any observable is easy to correct. This rescaling of the P-function somewhat increases the statistical error, but for systems with a small number of central spins this is not a problem.

The real difficulty comes from the fact that the analytics described above cannot be implemented exactly, which makes the approach approximate. Namely, the equations of motion (20) lead to the appearance of higher-order spherical harmonics in the function $P(\{\theta_j, \phi_j\}, t)$, i.e. such terms as $c_0^\alpha c_0^\beta c_k^\lambda c_k^\nu$ emerge. These terms do not directly affect $\rho(t)$ (they disappear after integration in equation (15)), but they contaminate the EOMs for physically relevant terms, so that the actual EOM for $w_{\gamma 0}(t)$ becomes $\ddot{w}_{\gamma 0}(t) = (A_k^2/2)(w_{0\gamma} - w_{\gamma 0}) + V$, where V is the contribution from the higher-order unphysical terms. The corresponding error is significant for small systems, with $N = 2$–5. However, real baths typically contain thousands of spins, and, fortunately, the error quickly decreases with increasing the total number of spins in the composite system. A large number of numerical examples (some of them are presented in section 3) show that, already for $N = 15$–20 spins, the P-representation simulations provide very accurate results for several experimentally important situations. However, extensive studies are still needed to understand in detail the limits of applicability of this approach.

Summarizing this section, we point out that a large number of methods are currently available for modelling spin-bath decoherence. The exact methods, such as the Suzuki–Trotter decomposition or the Chebyshev polynomial expansion, allow modelling of the systems with $N \sim 25$ spins on a single-processor workstation, and up to 30–40 spins by using larger computer systems. The main limitation of these approaches is that the required memory grows exponentially with N. More sophisticated methods employing the adaptive basis states, such as the TDMRG approach, allow modelling of even larger systems, up to 100–200 spins, but they

may become inefficient in some situations, when the number of relevant basis states grows too fast. Finally, for several experimentally important situations, the method based on P-representation sampling allows very accurate modelling of systems with $N = 10\,000$–$20\,000$ spins, but more extensive studies are needed to determine the usefulness of this method under different circumstances.

3. Applications to physical systems

The methods described above have been successfully applied for studying in detail a number of problems concerning the decoherence of spin systems by spin baths. Below, we describe several examples.

3.1. Decoherence of an electron spin in a quantum dot

Electron spins in quantum dots (QDs) have attracted much attention as possible building blocks for future applications in semiconductor coherent spintronics. In particular, QDs are considered as one of most promising candidates for implementation of quantum computations [66]. An electron spin localized in a quantum dot is well suited for representing a quantum bit (qubit): it is a natural two-state quantum system, which can be efficiently manipulated by external magnetic fields and gate voltages. QDs are also very promising as quantum spin memory units [67, 68]. The QD-based architectures are potentially scalable, and their fabrication relies on well-developed semiconductor technology. On the other hand, the electron spin is coupled to the phonons (via spin–orbit coupling) and to the large number of nuclear spins (e.g., for GaAs QDs, to the spins of ^{69}Ga, ^{71}Ga, and ^{75}As). For small and medium (less than $\sim$0.1 T) external fields and experimentally relevant (hundreds of mK) temperatures the hyperfine coupling with the nuclear spin bath leads to very quick decoherence, on a nanosecond time scale [8, 9, 69], and therefore constitutes a dominant decoherence channel (the phonon-induced decoherence becomes important at much larger fields [70–72]). Due to interaction with the bath of nuclear spins in a dot, the electron spin quickly 'loses memory' about its initial orientation and cannot be used for computation. Experimental studies of this process have become possible very recently [8–10], and detailed theoretical understanding of the experimental results is important. Moreover, the spin-bath decoherence of an electron spin in a quantum dot demonstrates a number of fundamentally interesting features, such as non-Markovian dynamics of the bath, which are important for general understanding of the decoherence process.

The Hamiltonian which describes an electron spin $\mathbf{S}_0$ interacting with a bath of N_B nuclear spins $\mathbf{S}_k$ ($k = 1, \ldots, N_\mathrm{B}$) in a QD includes many terms: (i) Zeeman energy of the electron spin; (ii) the isotropic contact hyperfine coupling between the electron and the nuclei; (iii) the Zeeman energy of the nuclear spins; (iv) the long-range electron–nuclei dipolar interaction and the anisotropic part of the hyperfine interaction arising from the dipolar electron–nuclear coupling; (v) the dipole–dipole coupling between the nuclear spins. However, on the nanosecond-to-microsecond timescale, which is of primary interest for us, only the first two terms are important, while the other interactions can be estimated to be 3–4 orders of magnitude smaller. Therefore, the relevant Hamiltonian is

$$H = g_e^* \mu_\mathrm{B} B_0 S_0^z + \sum_{k=1}^{N} A_k \mathbf{S}_k \mathbf{S}_0, \tag{23}$$

where B_0 is the external magnetic field, and $A_k = (8\pi/3) g_e^* \mu_\mathrm{B} g_n \mu_n u(\mathbf{r}_k)$ is the contact hyperfine coupling, determined by the electron density $u(\mathbf{r}_k)$ at the site $\mathbf{r}_k$ of the kth nuclear spin and by the Landé factors of the electron g_e^* and of the nuclei g_n.

We are interested in the dynamics of the central spin, i.e. in the dynamics of $\mathbf{s}_0(t) = \mathrm{Tr}\,\mathbf{S}_0\rho(t)$, where $\rho(t)$ is the composite density matrix. So far, an exact analytical solution of this problem has not been obtained. The Hamiltonian (23) is known to be integrable, but the formal solution [73] is very complex, and, to our knowledge, it has not yet been used for actual calculations of $s_0^z(t)$, in spite of recent progress in that direction [74]. Also, much research has been devoted to studying the situations where a large external magnetic field is applied, or where the nuclear spin bath has large polarizations. In these cases, the perturbation theory allows an extensive analysis [75–78]. But the interesting and experimentally relevant regime of moderate magnetic fields and/or moderate bath polarization is much more difficult to study by analytical means, and numerical simulations are important for detailed understanding of this situation.

The electron spin decoherence in a QD is an interesting two-step process [58, 69, 75–80]. At the same time, similar two-step decoherence was found for two coupled spins [36, 37]. The two-spin systems are under active theoretical investigation now [81, 82], but below we discuss only the single-spin case in order to focus on basic features of the decoherence process, thus keeping the presentation simple and accessible for a broader audience. The dynamics of an electron spin at short times and at long times is governed by different physical mechanisms, and different numerical approaches are needed to describe the short-time and long-time evolution of the system. The two stages will be considered in the next two subsections.

3.1.1. Short-time dynamics. Let us assume that initially the electron spin is prepared in the state $|\uparrow\rangle$, while the bath is completely disordered (unpolarized) and the corresponding density matrix is proportional to the unity matrix, $\rho_\mathrm{B} = 2^{-N_\mathrm{B}}\mathbf{1}$. In this case, the quantum-mechanical averages of the transverse components s_0^x and s_0^y remain zero throughout the evolution, but the dynamics of $s_0^z(t)$ is rather complex. In order to qualitatively understand the basic features of the decoherence process let us assume that $B_0 = 0$ and consider an unrealistic but exactly solvable case, when all coupling constants are equal to each other, $A_k = A$. In this case, the Hamiltonian (23) becomes $H = A\mathbf{S}_0\mathbf{S}$, where $\mathbf{S} = \sum_k \mathbf{S}_k$ is the total spin of the bath, and the problem can be easily solved:

$$s_0^z(t) = (1/6) + (1/3)(1 - 2b^2t^2)\exp(-b^2t^2) \tag{24}$$

where $b^2 = (1/8)\sum_k A_k^2 = A^2N_\mathrm{B}/8$. That is, the z-component of the electron spin first exhibits a Gaussian decay with the characteristic decoherence time $T_2^* = \sqrt{8/(N_\mathrm{B}A^2)}$, reaches the minimum, then increases and saturates at $1/6$. For a typical GaAs QD with the electron delocalized over $N = 10^6$ nuclear spins, $A \sim A_0/N \sim 10^{-4}$ μeV (where $A_0 \approx 0.1$ meV is the hyperfine coupling for an electron localized on a single nucleus [83]). The corresponding decoherence time $T_2^* \sim 10$ ns, as confirmed by recent experiments [8].

This analytical solution is possible because we neglected the dynamics of the bath. The assumption $A_k = A$ means that the 'length' of the total bath spin $\sqrt{\mathbf{S}^2}$ remains constant, so that $\mathbf{S}_0$ and $\mathbf{S}$ just precess around their vector sum $\mathbf{J} = \mathbf{S}_0 + \mathbf{S}$. Since $N_\mathrm{B} \gg 1$, the vectors $\mathbf{J}$ and $\mathbf{S}$ practically coincide, which means that the direction of the vector $\mathbf{S}$ also remains almost constant in time. Therefore, we are dealing with a simple dephasing of the vector $\mathbf{S}_0$ by a static environment, and $s_0^z(t)$ decays due to averaging over different possible directions and lengths of the vector $\mathbf{S}$. In particular, if we replace the quantum bath spin $\mathbf{S}$ by a classical random magnetic field $\mathbf{B}$ with Gaussian distribution, and average over all possible realizations of $\mathbf{B}$, then the same answer (24) can be obtained.

One may hope that the same qualitative arguments are applicable also in the realistic case, when all A_k are different. Although in this case both the direction and the length of the bath spin $\mathbf{S}$ change, at short times these changes may be small and thus can be neglected, so that

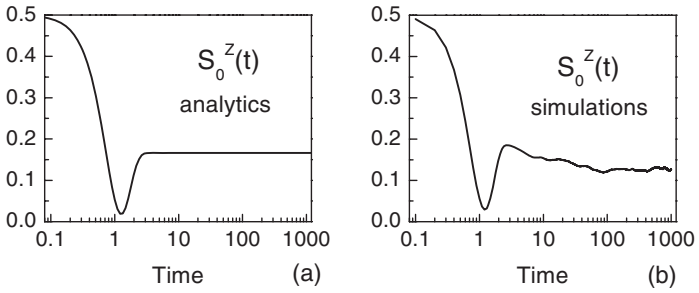

Figure 1. Time evolution of the z-component $s_0^z(t)$ of the electron spin interacting with $N_B = 21$ bath spins; the coupling constants A_k are random, uniformly distributed between 0 and 1. (a) The analytical result (24) obtained from the quasi-static bath approximation. (b) The result of numerical simulations performed using the Chebyshev polynomial expansion. At short times, $t \leqslant 5$, the agreement between approximate analytics and exact numerics is very good, while at longer times the slow logarithmic relaxation, not described by the QSA, takes place.

in the real QDs at short times one deals with the simple dephasing by a static bath. Such considerations form a basis for the quasi-static bath approximation (QSA), which has often been used to analyse the electron spin decoherence in QDs [8, 69, 76, 77, 82, 84]. The validity of these arguments has been verified by direct numerical simulations [80] for different magnetic fields B_0 and bath polarizations $P = M/(N_B/2)$ (where $M = \sum_k s_k^z$ is the magnetization of the bath). As an example, the results for $B_0 = P = 0$ are shown in figure 1. The quasi-static bath approximation agrees well with the exact numerical solution at short times. At longer times, however, $s_0^z(t)$ again slowly decreases with time, while the QSA predicts saturation at the value of $1/6$. The decrease of $s_0^z(t)$ at long times is qualitatively different: it is governed by the motion of the bath spins, and is beyond the QSA.

The QSA can be used to understand how the decoherence dynamics changes with external field and with the bath polarization. This approximation can be implemented in two equivalent ways, which lead to the same answer: either by considering the motion of a single central spin in a random external field, or by letting $A_k = A$ in the Hamiltonian (23) and solving the corresponding many-spin quantum problem. For the case of zero polarization and non-zero magnetic field, it gives

$$s_0^z(t) = (1/2) - W(\lambda, D; t), \tag{25}$$

and the function $W(\lambda, D; t)$ has the form

$$W = \frac{D}{\lambda^2} - \frac{D}{\lambda^2}\,\mathrm{e}^{-Dt^2/2}\cos\lambda t + \mathrm{i}\sqrt{\frac{\pi}{2}}\,\frac{D^{3/2}}{2\lambda^3}\,\mathrm{e}^{-\lambda^2/2D} \times \left[\Phi\left(\frac{Dt - \mathrm{i}\lambda}{\sqrt{2D}}\right) - \Phi\left(\frac{Dt + \mathrm{i}\lambda}{\sqrt{2D}}\right) + 2\Phi\left(\frac{\mathrm{i}\lambda}{\sqrt{2D}}\right)\right] \tag{26}$$

where $D = N_B/4$, and $\Phi(x)$ is the error function. For simplicity of notation, in these equations we took $A = 1$, and introduced the variable $\lambda = g_e^*\mu_B B_0/A$; this corresponds to normalization of the energy and time scales, so that the time t is measured in the units of $1/A$. In a similar way, we can consider the case of zero magnetic field and non-zero bath polarization $P \neq 0$. We assume that the initial state of the bath is described by the density matrix $\rho_B = (1/Z_\beta)\exp(-\beta M)$, where β is the inverse spin temperature of the bath, $M = \sum_k s_k^z$ is the bath magnetization, and $Z_\beta = [2\cosh(\beta/2)]^{N_B}$ is the statistical sum. Such a choice corresponds to a thermally polarized bath with the polarization $P = -\tanh(\beta/2)$, and

we are interested here in the case of small-to-moderate P. In this situation, the QSA gives

$$s_0^z(t) = (1/2) - W(\kappa, D; t), \tag{27}$$

where $\kappa = D\beta = N_B\beta/4$, and the function $W(\kappa, D; t)$ is defined by equation (26). It is also possible to obtain an analytic solution for large polarizations (when $P \sim 1$), but the answer is rather complex, and we do not present it here.

The validity of the quasi-static bath approximation can be checked by exact numerical simulations, using for example the Chebyshev polynomial expansion. The initial state of the composite system can be taken as $|\Psi(0)\rangle = |\uparrow\rangle \otimes |\chi_\beta\rangle$, where $|\uparrow\rangle$ describes the initial state of the electron spin, and the state $|\chi_\beta\rangle$ of the bath is designed to correspond to the density matrix $\rho_B = (1/Z_\beta)\exp(-\beta M)$. For $\beta = 0$, when $\rho_B = 2^{-N_B}\mathbf{1}$, the state $|\chi_0\rangle$ should be chosen as a normalized random state. Namely, we take the orthonormal basis $|Y_a\rangle$ for the bath, constructed as a product of the individual bath spin states, $|Y_a\rangle = |\alpha_{N-1}\alpha_{N-2}\ldots\alpha_1\rangle$, where $\alpha_k = 1$ if the kth spin is in the state 'up' and $\alpha_k = 0$ if this spin is in the state 'down'; there are $M_B = 2^{N_B}$ such basis states in total. The bath's state $|\chi_0\rangle$ is represented in this basis as

$$|\chi_0\rangle = \sum_{a=1}^{M_B} B_a|Y_a\rangle \tag{28}$$

where B_a are the independent, uniformly distributed random complex numbers, satisfying the normalization condition $\sum_a |B_a|^2 = 1$. In the corresponding density matrix $\rho'_B = |\chi_0\rangle\langle\chi_0|$, the diagonal elements are of order of 2^{-N_B}, while the off-diagonal elements are much smaller, of order of $2^{-N_B}/\sqrt{M_B}$, so that the matrix ρ'_B is almost proportional to the unity matrix, $\rho'_B = |\chi_0\rangle\langle\chi_0| \approx \rho_B = 2^{-N_B}\mathbf{1}$. For a sufficiently large number of bath spins, $N_B \sim 12$–14, a single realization of B_a is already sufficient to calculate the central system properties: after propagation in time and tracing out the bath spins, the random bath state gives an excellent approximation (with the negligible error of order of $1/\sqrt{M_B} = 2^{-N_B/2}$) for the central spin component $s_0^z(t)$. This fact has been known for quite a while in the computer physics community, and is based on solid mathematical arguments (Levy's lemma; see e.g. [85]). Furthermore, the random bath state is a starting point for modelling of the polarized bath. The state $|\chi_\beta\rangle$, which corresponds to the density matrix $\rho_B = (1/Z_\beta)\exp(-\beta M)$ for finite β, can be obtained from the random bath state $|\chi_0\rangle$ by applying the operator $V_\beta = \exp(-\beta\sum_k S_k^z)$ and subsequent normalization. The operator V_β can be implemented by using the imaginary-time extension of the Suzuki–Trotter or the Chebyshev polynomial method.

The evolution of $s_0^z(t)$ given by the QSA is shown in figure 2 for several different values of λ and κ, along with the corresponding numerical simulations. The quasi-static bath approximation demonstrates good agreement with the exact numerical results at short times. It is interesting that the functional form of equations (27) and (25) is identical, up to replacing κ by λ. The small nonzero bath polarization P affects the central spin in exactly the same way as the external field of the magnitude $B_0 = -PAN_B/(2g_e^*\mu_B)$, which is the average Overhauser field exerted on the central spin by the nuclear bath.

One may expect that by polarizing the bath, and therefore creating a more ordered initial state of the nuclear subsystem, the decoherence can be suppressed, i.e. the decoherence time may be increased. However, both analytics (QSA) and numerics show that this does not happen for experimentally relevant small-to-intermediate bath polarizations. The decoherence time is determined by the spread in the Overhauser fields, which is proportional to the variation of the bath magnetization $\langle(\Delta M)^2\rangle = (1 - P^2)N_B/4$, and is little affected by small bath polarizations P. Currently, strongly polarized baths are difficult to achieve experimentally, and such methods as narrowing the nuclear spin distribution [86], dynamical decoupling and spin echo techniques [8, 9, 87, 88] may be more practical for the suppression of decoherence.

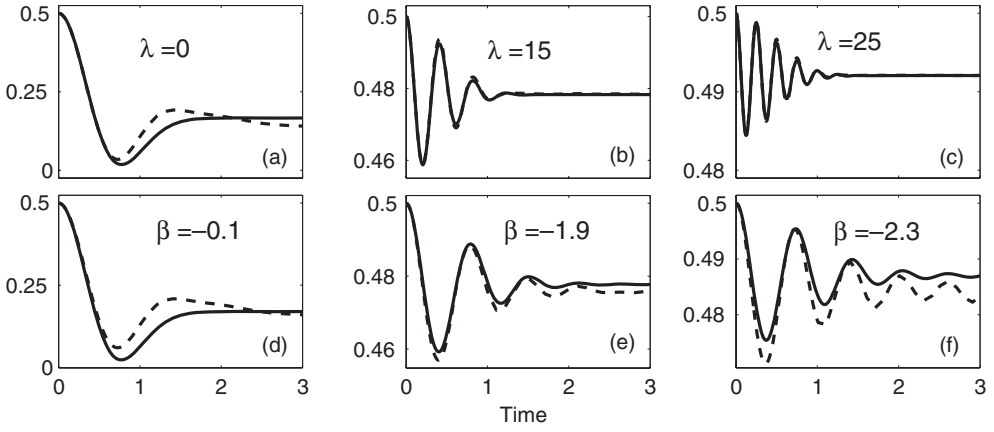

Figure 2. Time evolution of the z-component $s_0^z(t)$ of the electron spin interacting with $N_B = 20$ bath spins for different magnetic fields ((a)–(c)) and for different bath polarizations ((d)–(f)). The coupling constants A_k are random, uniformly distributed between 0 and 1. The dashed curves denote the exact numerical simulations results for $N = 20$, and the solid curves correspond to the analytical results obtained within the QSA. The numerical results agree well with the analytical predictions, and the underdamped oscillations appear once λ or κ is larger than $\sqrt{N}$.

Instead of suppressing decoherence, an increase of the magnetic field (and/or bath polarization) leads to the appearance of oscillations in $s_0^z(t)$ once the field exceeds a critical value, of order of $A_0(\sqrt{N_B}g_e^*\mu_B)^{-1}$, or when the polarization becomes larger than $1/\sqrt{N_B}$. This transition from smooth overdamped decay to underdamped oscillations is similar to the well-known transition in the dynamics of a damped oscillator: the evolution of the central spin is overdamped (or underdamped) depending on whether the decay time T_2^* is larger (or smaller) than the 'bare' oscillation frequency determined by λ or κ. In order to observe these oscillations in a typical GaAs quantum dot, a very modest external field of order of 3 mT, or polarization of order of 0.5%, is needed.

3.1.2. Long-time dynamics. In contrast with the short-time dynamics, the behaviour of an electron spin in a QD at long times is not yet understood in detail. Perturbation theory can be used to study the case of a strong magnetic field or strongly polarized nuclear spin bath [75, 77, 78], but for the experimentally important non-perturbative regimes, no well-justified analytical method has been suggested yet, and the interesting long-time dynamics of the central spin remains an open problem. The exact numerical simulations are also badly suited for such an investigation. The simulations with the baths of different sizes, varying from $N_B = 10$ to 24, show that $s_0^z(t)$ saturates at long times, and the saturation value steadily decreases with N_B. In order to obtain conclusive results, one needs to model the decoherence with thousands of bath spins, which is way beyond the capabilities of the exact simulations.

The coherent-state approach, as described in section 2.2, was developed to treat this problem [58]. As shown in figure 3, P-representation sampling gives excellent accuracy already for $N_B = 20$, and its accuracy only decreases with growing N_B. At $t = 0$, the composite density matrix $\rho(0) = 2^{-N_B}|\uparrow\rangle\langle\uparrow| \otimes \mathbf{1}$ corresponds to the P-function $P = (4\pi)^{-N}(1+3\cos\theta_0)$, which is not positively definite. According to section 2.2, the simulations are performed with the initial distribution $P' = (4\pi)^{-N}(1+\cos\theta_0)$, and $s_0^z(t)$ is calculated as an average:

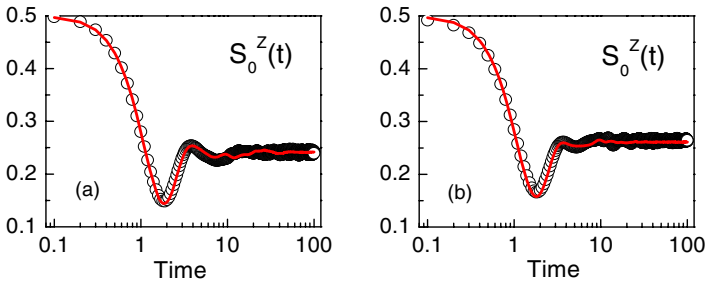

Figure 3. Longitudinal relaxation $s_0^z(t)$ of the central spin coupled to a bath of nuclear spins; the couplings A_k are randomly distributed between -0.4 and 0.6, the external field $g_e^*\mu_B B_0 = 1.0$. (a) central spin $1/2$, $N = 21$ bath spins (b) central spin 1, $N = 19$ bath spins. Solid lines denote the results of the exact solutions, the open circles denote the P-representation sampling results; the accuracy of the latter is excellent.

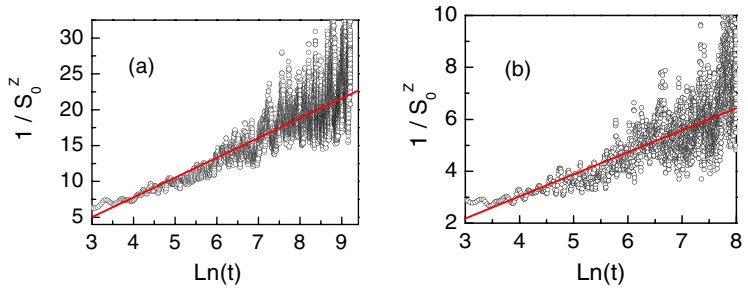

Figure 4. Long-time relaxation of the electron spin coupled to a bath of 16 000 nuclear spins $1/2$. Graphs show $1/s_0^z(t)$ as a function of $\ln t$. The coupling constants were calculated as $A_k = (1/14)u(\mathbf{r}_k)$, where $u(\mathbf{r})$ is the electron density. (a) $u(\mathbf{r})$ is taken as a Gaussian with the half-widths $d_x = 8.4a$, $d_y = 9.1a$, $d_z = 2.2a$ (a is the lattice constant), shifted from the centre of the lattice by the vector $(0.252a, 0.448a, 0.1a)$; (b) $u(\mathbf{r})$ is taken as an exponential function of $\mathbf{r}$, with the same parameters. An extra averaging over 20 neighbouring time points was used to decrease the number of realizations. The red solid lines are obtained from raw data.

$$s_0^z(t) = (1/2)\int 3\cos\theta_0\ P'(\{\theta_j, \phi_j\}, t)\prod_{j=0}^{N-1}\sin\theta_j\,\mathrm{d}\theta_j\,\mathrm{d}\phi_j. \tag{29}$$

Using the P-representation approach, electron spin decoherence has been modelled in a rather realistic setting [58]. The bath spins $1/2$ are assumed to be placed at the sites of a piece of a cubic lattice with the size $N_x \times N_y \times N_z$, ($N_x = N_y = 40$, $N_z = 10$, so the total number of bath spins $N_B = N_x N_y N_z = 16\,000$). The values of the hyperfine coupling constants A_k were chosen to be proportional to the electron density $u(\mathbf{r}_k)$ at the site $\mathbf{r}_k$ of the kth nuclear spin. The simulations were performed for two forms of the function $u(\mathbf{r}_k)$: (1) Gaussian with the half-widths $d_x = 8.4a$, $d_y = 9.1a$, $d_z = 2.2a$ along the x-, y-, and z-axes, correspondingly (where a is the lattice parameter), shifted from the centre of the lattice by the vector $(0.252a, 0.448a, 0.1a)$; (2) exponential with the same parameters. The corresponding simulations results are given in figure 4. Also, the simulations were done for a random set of A_k chosen from a uniform distribution. In all these cases, the numerical results suggest that at long times $s_0^z(t)$ exhibits a very slow logarithmic decay, $s_0^z(t) \sim 1/\ln t$.

Although the numerical results give strong evidence in support of such an unusual decay, this form has not yet been obtained analytically. The decay $1/\ln t$ was predicted from the

perturbation theory for polarized baths [75] in the case of a two-dimensional (2D) dot with Gaussian electron density, but other forms of decay have been predicted for other electron density distributions. In contrast, the P-representation modelling suggests $1/\ln t$ decay for different electron density distributions and for unpolarized baths. Also, similar relaxation was found [79] for a 2D Gaussian electron density, using the adiabatic approximation applied to the semiclassical EOM. The accuracy of this method is unclear; it is supposed to be correct for large N_B, but it is difficult to confirm or reject that: for $N_B = 22$ the exact solution disagrees with the approximation of [79], and for larger N_B the exact numerical solution is extremely difficult. Also, dependence of the long-time dynamics of the electron spin on the external magnetic field and on the bath polarization has not been studied yet.

3.2. Modelling of NMR experiments

Nuclear magnetic resonance (NMR) spectroscopy is an important tool widely used in physics, chemistry, and biology [16, 17]. By creating a non-equilibrium magnetization in a given group of nuclear spins (which have close Larmor frequencies), and by observing decay of this non-equilibrium magnetization, it is possible to obtain much knowledge about the interaction of these spins with each other, with other spins present in the sample, and with other external degrees of freedom. The shape and the characteristic decay time of the NMR signal, which is proportional to the non-equilibrium magnetization, are determined by the Hamiltonian which governs the dynamics of the given group of spins. Correspondingly, the parameters of this Hamiltonian (for instance, the strength of the coupling between the spins) can be found by analysing the time dependence of the NMR signal. For a small number of relevant spins (e.g., for a pair of spins), the Hamiltonian parameters can be relatively easily determined by analytical means. However, in more complex situations, numerical modelling of large spin systems is needed for detailed understanding of the NMR data.

Decoherence is the central process in the NMR experiments, which determines the decay of the signal [16, 17, 89, 90]. In some cases, however, identification of the central system and the bath is not completely trivial. In particular, below we focus on the systems of N identical spins $\mathbf{S}_k$ ($k = 1 \ldots N$) coupled by dipolar interactions: in such a system, every spin belongs to the central system and to the bath simultaneously, as follows. For a standard NMR experiments performed in a high quantizing field B_0 (several Tesla) directed along the z-axis, and at not-too-low temperatures (more than a few milliKelvins), the equilibrium density matrix is typically written in the form $\rho = (1/Z)\exp[-(\gamma\hbar B_0/T)\sum_k S_k^z] \approx \mathbf{1} - (\gamma\hbar B_0/T)\sum_k S_k^z$, where Z is the statistical sum, γ is the gyromagnetic ratio, and T is the temperature, which is much larger than $\gamma\hbar B_0$. By assuming this form, we have neglected other terms (the chemical shifts, the dipolar interactions, etc) which are much smaller than the 'bare' Zeeman energy. The first term (the unity matrix) in ρ is irrelevant: it does not change during the evolution, and also does not contribute to the NMR signal. Therefore, the relevant part of the density matrix is $\tilde{\rho} \propto \sum_k S_k^z$. The non-equilibrium magnetization along the x-axis is created by applying a $\pi/2$-pulse along the y-axis, which transforms S_k^z into S_k^x. Thus, the relevant part of the resulting density matrix acquires a form

$$\tilde{\rho} \propto S_1^x \otimes \mathbf{1}_2 \cdots \otimes \mathbf{1}_N + S_2^x \otimes \mathbf{1}_1 \otimes \mathbf{1}_3 \cdots \otimes \mathbf{1}_N + \cdots. \tag{30}$$

The first term in this sum corresponds to a composite density matrix, where the central system is made of the spin number 1 polarized along the x-axis, and a completely disordered bath is made of spins $2, 3, \ldots, N$. The second term corresponds to a central system made of the spin number 2 polarized along the x-axis, and a bath made of spins $1, 3, 4, \ldots, N$, and so on. Every spin is decohered by a bath made of all other spins, and the total NMR signal is the sum of individual contributions from all spins.

NMR experiments constitute an excellent testbed for decoherence studies. The nuclear spins are well isolated from the environment, and interactions which lead to a very fast decoherence in other systems are very weak in systems made of nuclear spins. The single-spin and many-spin coherences can persist for milliseconds in NMR experiments and therefore can be (relatively) easy to detect and analyse. It is not surprising that for example the first proof-of-concept implementation of quantum computations were performed using NMR techniques [7], and modern decoherence studies widely employ the concepts borrowed from spin resonance. The numerical methods described in section 2 are well suited for modelling the NMR experiments. Below, we present two examples of such modelling.

3.2.1. Spin echo in systems of dipolar-coupled spins. Spin echo is one of most amazing effects in spin resonance, which has determined the success of NMR techniques in a wide range of applications [16, 17, 91]. It is often the case that the decay of the nuclear magnetization is caused not by some physically interesting interaction, but comes from dephasing of nuclear spins by a parasitic static random field. By applying a π-pulse, the evolution of the nuclear spins in this static field can be reversed, so that the effect of dephasing is cancelled. The nuclear spins are refocused, and the NMR signal grows back to its original value exhibiting a sharp peak (the echo signal). Although the echo signal also decays in time, this decay is much slower, and it is caused not by parasitic fields but by physically important interactions. Development of these ideas has led to the appearance of a whole family of new methods, the dynamical decoupling techniques [87], which are used in various quantum systems in order to suppress unwanted interactions [92]. Much progress has been achieved in this area during the last three decades, but many issues have not been completely resolved yet. The behaviour of a real physical many-spin system subjected to a series of the control pulses can be very complex, and can exhibit very surprising features.

In particular, unusual results were obtained recently while studying the spin echo in silicon [93]. The spin echo decay was measured by two methods. First, regular Hahn echo experiments were performed. Initially, a non-equilibrium magnetization along the x-axis was created by applying a preparatory $\pi/2_Y$ pulse. The system was left to evolve freely for a time period τ, and then a refocusing π_X pulse was applied to the sample. After the time period τ following the refocusing pulse, an echo signal appears, and its height as a function of the time delay τ was recorded. In the second batch of experiments, instead of performing many measurements with different time delays, a Carr–Purcell–Meiboom–Gill (CPMG) refocusing sequence was used, i.e. a train of π_X pulses separated by the time delay 2τ was applied to the sample, and the decay of the echo signal was measured stroboscopically, after every pulse. Surprisingly, the echo decay in the second case was very different. For short τ, the CPMG echoes exhibited a very long tail, i.e. after some time, the decay of the CPMG echo was much slower than the decay of the Hahn echo. For larger delay times, along with the long-time tail, an interesting asymmetry in the echo signals was observed: every odd-numbered echo was noticeably smaller than every even-numbered echo. In subsequent experiments [94], such a difference was observed in many systems, from silicon with different dopants to yttrium oxide and fullerene samples, and the standard explanations (such as the diffusion of nuclei, which leads to similar consequences in liquid-state NMR) could not resolve the problem.

The only common feature for all solid-state systems where the difference between the Hahn echo and the CPMG echo has been detected is the presence of many nuclear spins coupled by dipolar interactions. Therefore, the relevant Hamiltonian can be assumed to have a well-known form (in the rotating frame, which will be used everywhere below),

$$H = \sum_k \hbar\omega_k S_k^z - \sum_{j>k} (A_{jk}/2)(\mathbf{S}_j\mathbf{S}_k - 3S_j^z S_k^z). \tag{31}$$

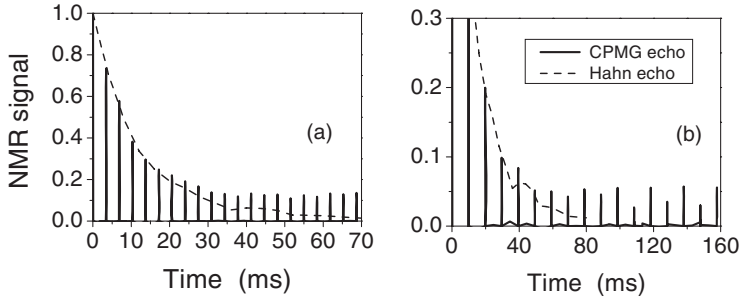

Figure 5. The calculated decay of spin echoes in a system of $N = 15$ dipolar coupled spins in silicon. In both panels, for reference, the dashed line shows the amplitude of Hahn echo as a function of total time t passed since the end of the preparatory $\pi/2_Y$ pulse. The solid line shows the NMR signal for CPMG echo as a function of total time t passed since the end of the preparatory $\pi/2_Y$ pulse. (a) The CPMG echo for inter-pulse delay $2\tau = 3.412$ ms; (b) the CPMG echo for inter-pulse delay $2\tau = 9.836$ ms.

The first term takes into account the random chemical shifts ω_k for the spins, and the second term describes the dipolar interactions with the coupling constants $A_{jk} = \gamma^2\hbar^2(1 - 3\cos^2\theta_{jk})/r_{jk}^3$, where θ_{jk} is the polar angle of the vector connecting the jth and the kth spins and r_{jk} is the length of this vector. The problem now becomes clear: every π_X pulse changes the sign of the first term, thus refocusing the rotation caused by the chemical shift, but leaves the dipolar part of the Hamiltonian intact. Therefore, the Hahn echo and the CPMG echo should decay in exactly the same manner, in contrast with the experimental results.

However, real π_X pulses are never ideal: the actual evolution of spins always slightly differs from the exact rotation described by the operator $U_p^0 = \exp(\mathrm{i}\pi \sum_k S_k^x)$. The pulse errors come from many sources: small inaccuracies in the pulse duration, from the transients at the front and tail of the pulse, etc. Some of the effects caused by the pulse non-idealities can be studied analytically, using various perturbative techniques [91, 95]. However, for more detailed understanding, numerical simulations are needed. As we show below, some of the experimentally observed effects may be qualitatively explained by the pulse errors, although a complete quantitative explanation of the experiments is still lacking.

To be specific, let us focus on the spin echo in the Si:P powder sample marked as the sample (d) in [93]. The exact simulations with $N = 15$ spins were performed using the Chebyshev polynomial expansion method. The only isotope of silicon having non-zero nuclear spin is ^{29}Si with spin $S = 1/2$, natural abundance 4.68%. Correspondingly, in numerical simulations, the spins $1/2$ were randomly placed in the sites of diamond lattice (the experimental value for the lattice constant $a = 5.43$ Å was taken) with the filling factor 4.68%. Orientation of the crystal lattice with respect to the quantizing field was chosen to be uniform, as expected in an unoriented powder sample, and the set of dipolar coupling constants A_{jk} was calculated. The spread in the chemical shifts ω_k is known from the free induction decay (FID) experiments; accordingly, in the simulations ω_k were drawn from the Gaussian distribution with FWHM $\Omega/2\pi = 3$ kHz. The simulation results were averaged over 10^2–10^3 realizations, each realization having a different set of ω_k, different configuration of nuclear spins and different orientation with respect to the quantizing field (i.e. different set of A_{jk}). The π_X pulses were assumed to have rectangular shape, and the strength of the pulse field H_1 was taken from experiments, $\gamma H_1/2\pi = 22$ kHz.

The typical simulations results are presented in figure 5, where the calculated Hahn echo decay, and the CPMG echo decay for both small and large inter-pulse delay, are shown. The

decay of the Hahn echo obtained from the simulations is in a reasonable agreement with experiments, the main source of error being the relatively small number N of spins, and does not exhibit any unusual features. However, after application of many consecutive π_X pulses, as in the CPMG experiments, the decay of the echo becomes much slower, and the long-time tail appears. Therefore, in agreement with experiments, the simulations demonstrate the clear difference between the Hahn echo and the CPMG echo. Moreover, when the inter-pulse delay time increases, a clear difference in height (about a factor of two) between the even-numbered and the odd-numbered echoes appears, also in agreement with the experimental findings.

The unusual behaviour of the CPMG echo is caused by the accumulation of small pulse errors. For the model considered above, these errors come from small but non-zero chemical shifts: since $\gamma H_1/\Omega \approx 7$, the contribution of the chemical shifts during the pulse are important. Instead of ideal rotation $U_p^0 = \exp(\mathrm{i}\pi S_k^x)$, the real evolution of the kth spin during the pulse is described by the operator $U_p = \exp[\mathrm{i}(\pi S_k^x + \xi_k S_k^z)]$, where $\xi_k = \omega_k/(\gamma H_1)$. Therefore, the rotation is non-uniform, and, after every pulse, the spins change orientation with respect to each other. As a result, the dipolar field created on a given spin by all other spins is reduced (see the explanations at the beginning of this section), and this leads to suppression of the dipolar interactions which determine the decay of the echo signal. Correspondingly, the decay of the CPMG echo becomes slower. The even–odd echo asymmetry can also be understood from this point of view: every π_X pulse flips a given spin, and only after an even number of pulses does the spin come back close to its initial orientation, so even-numbered echoes are higher than the odd-numbered ones.

The behaviour of the CPMG echo described above has some similarity with spin locking [96]. Although such an explanation is very tempting, experiments with an alternating-phase CPMG sequence give strong evidence against such an interpretation [93]. Also, the spin locking effect can be refuted by numerical modelling, by assuming that during the pulses every spin has its own effective rotation axis in the x–y plane. No spin locking can happen in this case, since the total locking field is zero, but the unusual features of the CPMG echo persist. Similarly, by performing simulations with time-varying chemical shifts $\omega_k(t)$ (modelled as Ornstein–Uhlenbeck processes with the correlation time t_c), it is possible to show that the long echo tail and the even–odd asymmetry become less pronounced as t_c becomes smaller.

The exact numerical calculations with $N = 15$ spins achieve a good qualitative description of the experiments, but for quantitative agreement, simulations with much larger N are required. Moreover, such simulations are needed to understand the experiments where stronger pulse fields H_1 have been used, $\gamma H_1/\Omega \sim 100$. For large H_1, the unusual features of the CPMG echo are still present, but the simulations with $N = 15$ cannot reproduce them. Realistic-size modelling with thousands of spins is yet to be performed; the coherent-state approach is a good candidate for such calculations, and applicability of this method for the NMR simulations has been verified very recently, as described below.

3.2.2. Free induction decay in CaF_2. The P-representation sampling described in section 2.2 is a rather natural candidate for modelling large quantum spin systems, as needed for numerical simulations of the NMR experiments. This method has been successfully applied for studying the decoherence of electron spins in quantum dots, but its accuracy is hard to estimate analytically, and it is not clear *a priori* whether the P-representation simulations give sufficiently accurate results for complex systems involving a large number of spins coupled by dipolar interactions.

The simplest way to validate the method is to compare the simulation results with the experimental data obtained for a suitable reference system. For solid-state NMR, single crystals of calcium fluoride CaF_2 constitute a good choice: large clean crystals can be relatively easily

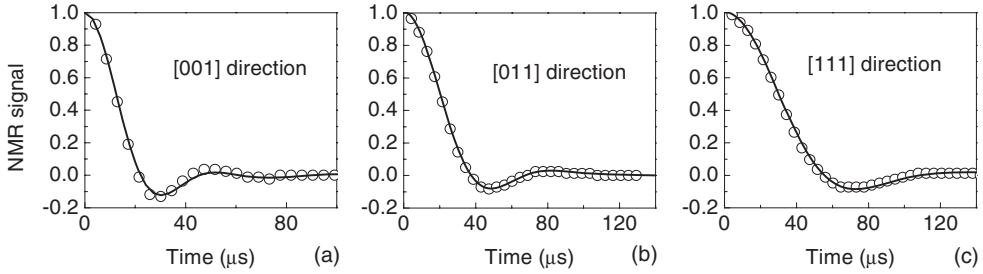

Figure 6. The free induction decay in a single crystal of CaF_2 for different orientations of the quantizing axis: (a) [001]; (b) [011]; (c) [111]. Solid lines denote the simulation results obtained using the P-representation sampling with no fitting parameters, and the empty circles denote the experimental data obtained in [97].

grown, and the free induction decay (FID) in CaF_2 was measured with excellent accuracy a long time ago [97]. The nuclear spins of fluorine ($S = 1/2$ with 100% natural abundance) are placed in the sites of a simple cubic lattice with the lattice constant $a = 2.723$ Å, while the nuclear spins of ^{43}Ca are rare (0.135% abundance) and their influence can be neglected.

The evolution of the fluorine spins in clean crystals of CaF_2 can be described by the dipolar Hamiltonian

$$H = \sum_{j>k} (A_{jk}/2)(3S_j^z S_k^z - \mathbf{S}_j \mathbf{S}_k), \tag{32}$$

with the coupling constants $A_{jk} = \gamma^2\hbar^2(1 - 3\cos^2\theta_{jk})/r_{jk}^3$, where θ_{jk} is the polar angle of the vector connecting the jth and the kth spins and r_{jk} is the length of this vector. All other interactions are very small and can be neglected. The equations of motion for $\mathbf{C}_j(t)$ can be derived in complete analogy with section 2.2, and give an analogous result:

$$\dot{\mathbf{C}}_j = [\mathbf{h}_j \times \mathbf{C}_j] \tag{33}$$

where the components of the local field $\mathbf{h}_j$ are $h_j^x = -(\sqrt{3}/4)\sum_k A_{jk} S_k^x$, $h_j^y = -(\sqrt{3}/4)\sum_k A_{jk} S_k^y$, and $h_j^z = (\sqrt{3}/2)\sum_k A_{jk} S_k^z$. Due to translational invariance, the coupling coefficients A_{jk} depend only on $\mathbf{r}_{jk} = \mathbf{r}_j - \mathbf{r}_k$, so the expressions for the local fields $\mathbf{h}_j$ have a form of discrete convolution, and can be efficiently calculated by fast Fourier transformation.

The calculations of the FID curves were performed for a piece of cubic lattice of size $30 \times 30 \times 30$, i.e. a total of $N = 27\,000$ quantum spins 1/2 were modelled. Free boundary conditions were assumed, and the zero padding method was used to calculate the convolutions via fast Fourier transforms. The initial distribution function $P(t = 0) = \prod_k P_k$ was chosen as a product of individual P-functions $P_k = (1 + p\sin\theta_k\cos\phi_k)$ with small $p = 0.05$, which corresponds to a system of spins slightly polarized along the x-axis. Although this corresponds to a slightly polarized bath (see equation (30)), the error introduced by such a choice is of order of p^2 and is very small. The NMR signal was calculated as $M^x/(pN/2)$, where $M^x(t) = \sum_k s_k^x(t)$ is the total nuclear magnetization along the x-axis.

The simulation results are presented in figure 6 for three different orientations of the quantizing field, along the axes [001], [011], and [111]. In all three cases the agreement between the simulations and the experiment is spectacularly good. The detailed shape of the FID curves in CaF_2 has been studied theoretically before [98] (beyond the calculation of the moments), but this theory requires several fitting parameters to be determined from the experimental data. To our knowledge, the P-representation simulations for the first time allow

very accurate modelling of the free induction decay in a solid-state NMR system with a very large number of spins without using any fitting parameters whatsoever. This result gives us hope that the P-representation sampling may be a suitable method for studying NMR in complex spin systems. However, much work is still needed to confirm or reject this hope.

4. Summary and future prospects

Above, we have outlined several most typical methods which have been used so far for modelling the decoherence of spin systems by spin baths. Among them, such exact methods as the Suzuki–Trotter decomposition and the Chebyshev polynomial expansion are the most versatile, and they can be used for modelling almost any type of system. Their most important drawback is that the total number of spins which these methods can handle is rather small, but they still can be very helpful for understanding the decoherence dynamics in various systems. Other exact methods, such as the TDMRG approach, can model much bigger systems, and have been successfully applied for studying many physically interesting situations. However, when the dynamics of the decoherence process is very complex, leading to strong entanglement between all spins in the composite system, the TDMRG approach may break down. Finally, approximate simulations based on the coherent-state representation of the density matrix demonstrate very high accuracy and have been successfully applied so far to several problems, but their limitations are not yet clear. Expanding this approach and studying its region of validity may lead to interesting results in the future.

In this review, we have considered only single-spin central systems, in order to keep the presentation simple. The decoherence process in systems containing few spins can already be very rich [36, 37, 81]. Moreover, the spin-bath decoherence of 'truly' many-spin systems, e.g. spin chains, can be even more interesting, due to interplay between the intra-system excitations and the coupling to the spin bath [99]. This area of research attracts more and more attention now [100], but still remains largely unexplored, in spite of its relevance for quantum computations and quantum communications.

Also, in this review we only briefly mentioned such a promising and important research direction as studying the dynamical decoupling methods designed for mitigating decoherence [87, 88, 92]. These methods employ specially constructed sequences of pulses which are applied to the central system in order to suppress the coupling to the decohering environment. Many such sequences have been developed in the context of NMR and ESR [16, 17, 91], but development of the dynamical decoupling methods for other systems requires much research [87, 92]. At the same time, the analytical tools are not always sufficient to study in detail the dynamics of an open central system subjected to time-varying magnetic fields. The numerical simulations can greatly facilitate the analysis of different decoupling methods, and can help a lot in assessing the performance of these methods for various types of spin bath. Also, as we considered above, numerical simulations may be very useful for studying the unavoidable imperfections of the decoupling methods (such as for example the pulse errors).

The new problems arising in the studies of decoherence will inevitably require the development of new numerical tools, and development of the simulation techniques may be important for further progress. In particular, it may be interesting to study the applicability of the MCTDH technique [49, 50] for modelling decoherence in those cases where the TDMRG approach breaks down. Another potentially promising approach is the further development of coherent-state approaches using the insights gained in quantum optics [18, 63–65]. Finally, it may be especially interesting to consider the possibility of combining the coherent-state simulations of the bath with the exact simulations of the central system.

Acknowledgments

The authors would like to thank S E Barrett, D G Cory, E Dagotto, H De Raedt, B N Harmon, M I Katsnelson, S A Lyon, C P Slichter, A M Tyryshkin, L Viola, and W Zurek for stimulating discussions. This work was supported by the NSA and ARDA under Army Research Office (ARO) contract DAAD 19-03-1-0132. This work was partially carried out at the Ames Laboratory, which is operated for the US Department of Energy by Iowa State University under contract No. W-7405-82 and was supported by the Director of the Office of Science, Office of Basic Energy Research of the US Department of Energy. This work was supported by the NSF grant No. DMR-0454504.

References

[1] Thomsen L K, Mancini S and Wiseman H M 2002 *Phys. Rev.* A **65** 061801(R)
[2] Geremia J M, Stockton J K and Mabuchi H 2005 *Phys. Rev. Lett.* **94** 203002
[3] Cappellaro P, Emerson J, Boulant N, Ramanathan C, Lloyd S and Cory D G 2005 *Phys. Rev. Lett.* **94** 020502
[4] Awschalom D, Loss D and Samarth N (ed) 2002 *Semiconductor Spintronics and Quantum Computations* (Berlin: Springer)
[5] Nielsen M A and Chuang I L 2000 *Quantum Computation and Quantum Information* (Cambridge: Cambridge University Press)
[6] Datta S and Das B 1990 *Appl. Phys. Lett.* **56** 665
[7] Vandersypen L M K, Steffen M, Breyta G, Yannoni C S, Sherwood M and Chuang I L 2001 *Nature* **414** 883
[8] Johnson A C, Petta J R, Taylor J M, Yacoby A, Lukin M D, Marcus C M, Hanson M P and Gossard A C 2005 *Nature* **435** 925
Petta J R, Johnson A C, Taylor J M, Laird E A, Yacoby A, Lukin M D, Marcus C M, Hanson M P and Gossard A C 2005 *Science* **309** 2180
[9] Koppens F H L, Folk J A, Elzerman J M, Hanson R, Willems van Beveren L H, Vink I T, Tranitz H P, Wegscheider W, Kouwenhoven L P and Vandersypen L M K 2005 *Science* **309** 1346
[10] Koppens F H L, Buizert C, Tielrooij K J, Vink I T, Nowack K C, Meunier T, Kouwenhoven L P and Vandersypen L M K 2006 *Nature* **442** 766
[11] Mamin H J, Budakian R, Chui B W and Rugar D 2003 *Phys. Rev. Lett.* **91** 207604
Budakian R, Mamin H J and Rugar D 2004 *Phys. Rev. Lett.* **92** 037205
[12] Kohn W and Luttinger J M 1957 *Phys. Rev.* **108** 590
Kohn W and Luttinger J M 1958 *Phys. Rev.* **109** 1892
[13] Imry Y 2002 *Introduction to Mesoscopic Physics* (Oxford: Oxford University Press)
[14] Altshuler B L, Aronov A G and Khmelnitskii D E 1981 *Solid State Commun.* **39** 619
Altshuler B L, Aronov A G and Khmelnitskii D E 1982 *J. Phys. C: Solid State Phys.* **15** 7367
[15] Sachdev S 1999 *Quantum Phase Transitions* (Cambridge: Cambridge University Press)
[16] Slichter C 1992 *Principles of Magnetic Resonance* (Berlin: Springer)
[17] Ernst R R, Bodenhausen G and Wokaun A 1987 *Principles of Nuclear Magnetic Resonance in One and Two Dimensions* (Oxford: Oxford University Press)
[18] Gardiner C W and Zoller P 2000 *Quantum Noise* (Berlin: Springer)
[19] Leggett A J, Chakravarty S, Dorsey A T, Fisher M P A, Garg A and Zwerger W 1995 *Rev. Mod. Phys.* **59** 1
[20] Blanchard Ph, Giulini D, Joos E, Kiefer C and Stamatescu I-O (ed) 2000 *Decoherence: Theoretical, Experimental and Conceptual Problems* (Berlin: Springer)
[21] Zurek W H 1981 *Phys. Rev.* D **24** 1516
Zurek W H 1982 *Phys. Rev.* D **26** 1862
[22] Joos E and Zeh H D 1985 *Z. Phys.* B **59** 223
[23] Caldeira A O and Leggett A J 1983 *Ann. Phys.* **149** 374
[24] Feynman R P and Vernon F L Jr 1963 *Ann. Phys.* **24** 118
[25] Stamp P C E 1995 Unconventional environments *Quantum Tunneling of Magnetization—QTM'94* (*NATO ASI Series E: Applied Sciences* vol 301) ed L Gunther and B Barbara (Dordrecht: Kluwer–Academic)
[26] Shao J and Hänggi P 1998 *Phys. Rev. Lett.* **81** 5710
[27] Schulten K and Wolynes P G 1978 *J. Chem. Phys.* **68** 3292

[28] Garg A 1993 *Phys. Rev. Lett.* **70** 1541
Garg A 1995 *Phys. Rev. Lett.* **74** 1458
[29] Prokof'ev N V and Stamp P C E 1996 *J. Low Temp. Phys.* **104** 143
Prokof'ev N V and Stamp P C E 2000 *Rep. Prog. Phys.* **63** 669
[30] Jalabert R A and Pastawski H M 2001 *Phys. Rev. Lett.* **86** 2490
Karkuszewski Z P, Jarzynski C and Zurek W H 2002 *Phys. Rev. Lett.* **89** 170405
Poulin D, Blume-Kohout R, Laflamme R and Ollivier H 2004 *Phys. Rev. Lett.* **92** 177906
Emerson J, Weinstein Y S, Lloyd S and Cory D G 2002 *Phys. Rev. Lett.* **89** 284102
Yuan S, Katsnelson M I and De Raedt H 2006 *JETP Lett.* **84** 99
[31] Lages J, Dobrovitski V V, Katsnelson M I, De Raedt H A and Harmon B N 2005 *Phys. Rev.* E **72** 026225
[32] Sinitsyn N A and Dobrovitski V V 2004 *Phys. Rev.* B **70** 174449
[33] Katsnelson M I, Dobrovitski V V, De Raedt H A and Harmon B N 2003 *Phys. Lett.* A **318** 445
[34] Ermann L, Paz J P and Saraceno M 2006 *Phys. Rev.* A **73** 012302
Jacquod Ph 2004 *Phys. Rev. Lett.* **92** 150403
Jacquod Ph, Silvestrov P G and Beenakker C W J 2001 *Phys. Rev.* E **64** 055203(R)
Georgeot B and Shepelyansky D L 2000 *Phys. Rev.* E **62** 6366
Georgeot B and Shepelyansky D L 1998 *Phys. Rev. Lett.* **81** 5129
[35] Prosen T and Žnidarič M 2003 *J. Phys. A: Math. Gen.* **36** 2463
Cerruti N R and Tomsovic S 2002 *Phys. Rev. Lett.* **88** 054103
Cucchietti F M, Lewenkopf C H, Mucciolo E R, Pastawski H M and Vallejos R O 2002 *Phys. Rev.* E **65** 046209
[36] Dobrovitski V V, De Raedt H A, Katsnelson M I and Harmon B N 2003 *Phys. Rev. Lett.* **90** 210401
[37] Melikidze A, Dobrovitski V V, De Raedt H A, Katsnelson M I and Harmon B N 2004 *Phys. Rev.* B **70** 014435
[38] Breuer H-P and Petruccione F 2002 *The Theory of Open Quantum Systems* (Oxford: Oxford University Press)
[39] Alicki R and Lendi K 1987 *Quantum Dynamical Semigroups and Applications* (Berlin: Springer)
[40] De Raedt H and Dobrovitski V V 2004 *Computer Simulation Studies in Condensed-Matter Physics XVI* ed D P Landau, S P Lewis and H-B Schüttler (Berlin: Springer)
[41] Dobrovitski V V and De Raedt H A 2003 *Phys. Rev.* E **67** 056702
[42] Suzuki M, Miyashita S and Kuroda A 1977 *Prog. Theor. Phys.* **58** 1377
[43] de Vries P and De Raedt H 1993 *Phys. Rev.* B **47** 7929
[44] De Raedt H, Hams A H, Michielsen K and De Raedt K 2000 *Comput. Phys. Commun.* **132** 1
[45] Tal-Ezer H and Kosloff R 1984 *J. Chem. Phys.* **81** 3967
Tal-Ezer H 1986 *SIAM J. Numer. Anal.* **23** 11
Tal-Ezer H 1989 *SIAM J. Numer. Anal.* **26** 1
[46] Kosloff R 1994 *Ann. Rev. Phys. Chem.* **45** 145
[47] Weisse A, Wellein G, Alvermann A and Fehske H 2006 *Rev. Mod. Phys.* **78** 275
Aliaga H 2005 *Phys. Rev.* B **71** 184404
Iitaka T, Nomura S, Hirayama H, Zhao X, Aoyagi Y and Sugano T 1997 *Phys. Rev.* E **56** 1222
Alvarez G and Schulthess T C 2006 *Phys. Rev.* B **73** 035117
[48] Suzuki M and Umeno K 1993 *Computer Simulation Studies in Condensed Matter Physics VI* ed D P Landau, K K Mon and H B Schüttler (Berlin: Springer)
[49] Beck M H, Jäckle A, Worth G A and Meyer H-D 2000 *Phys. Rep.* **324** 1
[50] Wang H 2000 *J. Chem. Phys.* **113** 9948
Thoss M, Wang H and Miller W H 2001 *J. Chem. Phys.* **115** 2991
[51] Feiguin A and White S R 2003 *Phys. Rev. Lett.* **93** 076401
[52] Vidal G 2003 *Phys. Rev. Lett.* **91** 147902
[53] Daley A J, Kollath C, Schollwöck and Vidal G 2004 *Preprint* cond-mat/0403313
[54] White S R 1998 *Phys. Rep.* **301** 187
[55] Gobert D, Kollath C, Schollwöck U and Schütz G 2005 *Phys. Rev.* E **71** 036102
[56] Binder K (ed) 1995 *The Monte Carlo Method in Condensed Matter Physics* (Berlin: Springer)
[57] De Raedt H and Lagendijk A 1981 *Phys. Rev. Lett.* **46** 77
[58] Al-Khassanieh K A, Dobrovitski V V, Dagotto E and Harmon B N 2006 *Phys. Rev. Lett.* **97** 037204
[59] Radcliffe J M 1971 *J. Phys. A: Math. Gen.* **4** 313
[60] Klauder J R and Skagerstam B-S 1985 *Coherent States* (Singapore: World Scientific)
[61] Glauber R J 1963 *Phys. Rev. Lett.* **10** 84
[62] Sudarshan E C G 1963 *Phys. Rev. Lett.* **10** 277
[63] Carusotto I and Castin Y 2001 *J. Phys. B: At. Mol. Opt. Phys.* **34** 4589
[64] Deuar P and Drummond P D 2002 *Phys. Rev.* A **66** 033812

Corney J F and Drummond P D 2004 *Phys. Rev. Lett.* **93** 260401
[65] Plimak L I, Olsen M K and Collett M J 2001 *Phys. Rev.* A **64** 025801
[66] Loss D and DiVincenzo D P 1998 *Phys. Rev.* A **57** 120
Imamoglu A, Awschalom D D, Burkard G, DiVincenzo D P, Loss D, Sherwin M and Small A 1999 *Phys. Rev. Lett.* **83** 4204
[67] Taylor J M, Marcus C M and Lukin M D 2003 *Phys. Rev. Lett.* **90** 206803
[68] Dobrovitski V V, Taylor J M and Lukin M D 2006 *Phys. Rev.* B **73** 245318
[69] Merkulov I A, Efros Al L and Rosen M 2002 *Phys. Rev.* B **65** 205309
[70] Elzerman J M, Hanson R, Willems van Beveren L H, Witkamp B, Vandersypen L M K and Kouwenhoven L P 2004 *Nature* **430** 431
[71] Woods L M, Reinecke T L and Lyanda-Geller Y 2003 *Phys. Rev.* B **66** 161318
[72] Khaetskii A V and Nazarov Yu V 2001 *Phys. Rev.* B **64** 125316
[73] Gaudin M 1976 *J. Physique* **37** 1087
Gaudin M 1983 *La fonction d'onde de Bethe* (Paris: Masson)
[74] Yuzbashyan E A, Altshuler B L, Kuznetsov V B and Enolskii V Z 2005 *J. Phys. A: Math. Gen.* **38** 7831
[75] Coish W A and Loss D 2004 *Phys. Rev.* B **70** 195340
[76] Schliemann J, Khaetskii A and Loss D 2003 *J. Phys.: Condens. Matter* **15** R1809
[77] Khaetskii A V, Loss D and Glazman L 2003 *Phys. Rev. Lett.* **88** 186802
[78] Deng C and Hu X 2006 *Phys. Rev.* B **73** 241303(R)
[79] Erlingsson S I and Nazarov Yu V 2004 *Phys. Rev.* B **70** 205327
[80] Zhang W, Dobrovitski V V, Al-Hassanieh K A, Dagotto E and Harmon B N 2006 *Preprint* cond-mat/0609185
[81] Coish W A and Loss D 2005 *Phys. Rev.* B **72** 125337
Erlingsson S I, Jouravlev O N and Nazarov Yu V 2005 *Phys. Rev.* B **72** 033301
Serebrennikov Yu A 2006 *Phys. Rev.* B **74** 035325
[82] Taylor J M, Petta J R, Johnson A C, Yacoby A, Marcus C M and Lukin M D 2006 *Preprint* cond-mat/0602470
[83] Paget D, Lampel G, Sapoval B and Safarov V I 1977 *Phys. Rev.* B **15** 5780
[84] Semenov Y G and Kim K W 2003 *Phys. Rev.* B **67** 073301
[85] Popescu S, Short A J and Winter A 2005 *Preprint* quant-ph/0511225
[86] Stepanenko D, Burkard G, Giedke G and Imamoglu A 2006 *Phys. Rev. Lett.* **96** 136401
[87] Viola L, Knill E and Lloyd S 1999 *Phys. Rev. Lett.* **82** 2417
Viola L and Knill E 2005 *Phys. Rev. Lett.* **94** 060502
Khodjasteh K and Lidar D A 2005 *Phys. Rev. Lett.* **95** 180501
Facchi P, Tasaki S, Pascazio S, Nakazato H, Tokuse A and Lidar D A 2005 *Phys. Rev.* A **71** 022302
[88] Shenvi N, de Sousa R and Whaley K B 2005 *Phys. Rev.* B **71** 224411
Witzel W M, de Sousa R and Das Sarma S 2005 *Phys. Rev.* B **72** 161306(R)
Yao W, Liu R-B and Sham L J 2006 *Preprint* cond-mat/0604634
Saikin S K, Yao W and Sham L J 2006 *Preprint* cond-mat/0609105
Witzhel W M and Das Sarma S 2006 *Phys. Rev.* B **74** 035322
[89] Cho H, Ladd T D, Baugh J, Cory D G and Ramanathan C 2005 *Phys. Rev.* B **72** 054427
[90] Cho H, Cappellaro P, Cory D G and Ramanathan C 2006 *Preprint* cond-mat/0608620
[91] Haeberlen U 1976 *High Resolution NMR in Solids: Selective Averaging* (New York: Academic)
[92] Morton J J L, Tyryshkin A M, Ardavan A, Benjamin S C, Porfyrakis K, Lyon S A and Briggs G A D 2006 *Nat. Phys.* **2** 40
Fraval E, Sellars M J and Longdell J J 2002 *Phys. Rev. Lett.* **95** 030506
Greilich A, Oulton R, Zhukov E A, Yugova I A, Yakovlev D R, Bayer M, Shabaev A, Efros Al L, Merkulov E A, Stavarache V, Truter D and Wieck A 2006 *Phys. Rev. Lett.* **96** 227401
[93] Dementyev A E, Li D, MacLean K and Barrett S E 2003 *Phys. Rev.* B **68** 153302
[94] Li D, Dong Y, Ramos R, Dementyev A and Barrett S 2006 *Bull. Am. Phys. Soc.* **51** R40.00002
Barrett S E 2005 private communication
Lyon S A and Tyryshkin A M 2005 private communication
[95] Gerstein B C and Dybowski C R 1985 *Transient Techniques in NMR of Solids* (New York: Academic)
[96] Rhim W-K, Burum D P and Elleman D D 1976 *Phys. Rev. Lett.* **37** 1764
Ivanov Yu N, Provotorov B N and Fel'dman E B 1978 *JETP Lett.* **27** 153
Erofeev L N and Shumm B A 1978 *JETP Lett.* **27** 149
Suwelack D and Waugh J S 1980 *Phys. Rev.* B **22** 5110
[97] Lowe I J and Norberg R E 1957 *Phys. Rev.* **107** 46
Engelsberg M and Lowe I J 1974 *Phys. Rev.* B **10** 822

[98] Fine B V 1997 *Phys. Rev. Lett.* **79** 4673
[99] Katsnelson M I, Dobrovitski V V and Harmon B N 2001 *Phys. Rev.* B **63** 212404
Katsnelson M I, Dobrovitski V V and Harmon B N 2000 *Phys. Rev.* A **62** 022118
[100] Among numerous works in this area, we mention only a few Khaneja N and Glaser S J 2002 *Phys. Rev.* A **66** 060301(R)
Bose S 2003 *Phys. Rev. Lett.* **91** 207901
Rossini D, Giovannetti V and Fazio R 2006 *Preprint* quant-ph/0609022
Jané E, Vidal G, Dür W, Zoller P and Cirac J I 2003 *Quantum Inf. Comput.* **3** 15